Angewandte Chemie
Eine Zeitschrift der Gesellschaft Deutscher Chemiker

Supporting Information

Expanding the Landscape of Diterpene Structural Diversity through Stereochemically Controlled Combinatorial Biosynthesis

*Johan Andersen-Ranberg, Kenneth Thermann Kongstad, Morten Thrane Nielsen, Niels Bjerg Jensen, Irini Pateraki, Søren Spanner Bach, Britta Hamberger, Philipp Zerbe, Dan Staerk, Jörg Bohlmann, Birger Lindberg Møller, and Björn Hamberger**

anie_201510650_sm_miscellaneous_information.pdf

Supplementary information

Table of Contents

Supplementary material

Supplementary table S1: genes used in this work. The biosynthetic function of previously characterized diTPS and their putative native function are illustrated in figure 2, in the main text. Diterpene synthase (diTPS), 1-deoxy-D-xylose 5-phosphate synthase (DXS), geranylgeranyldiphosphate synthase (GGPPS). Primers for isolation and cloning of the above genes are given in table S10. Cf, *Coleus forskohlii*; Ss, *Salvia sclarea*; Mv, *Marrubium vulgare*; Ep, *Euphorbia peplus*; Os, *Oryza sativa*; Tw, *Tripterygium wilfordii*; Zm, *Zea mays*.

Gene name	Type	Genbank accession number	Reference
CfTPS1	Class II diTPS	KF444506	[1]
CfTPS2	Class II diTPS	KF444507	[1]
CfTPS3	Class I diTPS	KF444508	[1]
CfTPS4	Class I diTPS	KF444509	[1]
CfTPS14	Class I diTPS	KC7022394	[2]
SsLPPS	Class II diTPS	JQ478434	[3]
SsSCS	Class I diTPS	JQ478435	[3]
MvCPS1	Class II diTPS	KJ584450	[4]
MvELS	Class I diTPS	KJ584454	[4]
EpTPS1	Class I diTPS	KC7022395	[2]
EpTPS7	Class II diTPS	KC7022396	[2]
EpTPS8	Class I diTPS	KP889107	This work
EpTPS23	Class I diTPS	KP889108	This work
OssynCPS	Class II diTPS	AY530101	[5]
TwTPS2	Class I diTPS	KP889109	This work
TwTPS7	Class I diTPS	KP889110	This work
TwTPS14	Class II diTPS	KP889111	This work
TwTPS21	Class II diTPS	KP889112	This work
TwTPS28	Class II diTPS	KP889113	This work
ZmAN2	Class II diTPS	AY562491	[6]
CfDXS	DXS	KP889115	This work
CfGGPPS	GGPPS	KP889114	This work

Diterpenes identified in the heterologous expression system *N. benthamiana*/Agrobacterium

Supplementary table S2. Compound overview. Identification (ID) levels follow a previous definition[7] and are summarized as follows. The ID level 1 requires a minimum of two independent orthogonal datasets to confirm the identity of the specific compound. In this work these orthogonal datasets represent comparison of mass spectrum to an authentic standard, retention time and NMR analysis by ^{1}H-NMR and/or ^{13}C-NMR. The ID level 2 is defined as compounds identified by comparison of retention index and MS spectrums to references described in literature and a reference library (National Institute of Standards and Technology MS (Wiley W9N08L)). An ID level of 3 is defined as putative diterpenes detected, established by the characteristic ions *m*/*z* 272 or *m*/*z* 275 for diterpene products in total ion chromatogram (TIC) peaks from the GC-MS analysis of all extracts. No diterpenes were detected in extracts from *N. benthamiana* expressing the silencing suppressor p19 (negative control).[8]

Diterpene	Name	RI	In combinatorial wheel (fig. 2)	NMR	Authentic standard	Confirmed *in vitro*	Production in yeast (titer)	ID Level
(1)	unknown	1906	no					3
(2)	pimara-8(14),15-diene	1923	no		yes			1
(3)	unknown	1938	no					3
(4)	unknown	1938	yes					3
(5)	9,13-epoxy-labd-14-ene	1952	yes		yes			1
(6)	*syn*-pimara-9(11),15-diene	1953	yes	table S8		yes, figure S10	yes	1
(7)	unknown	1957	no					3
(8)	unknown	1967	no					3
(9a/b)	(*+*)/*ent*-sandaracopimaradiene	1972	yes		yes	yes, figure S8		1
(10)	unknown	1975	yes					3
(11)	*syn*-manool	1981	yes	table S5	yes	yes, figure S12		1
(12)	unknown	1989	no					3
(13)	unknown	1994	no					3
(14)	unknown	1997	no					3
(15)	kaur-15-ene	2000	yes					2
(16a/b)	13*R*-(*+*)-manoyl oxide/ 13S-*ent*-manoyl oxide	2002	yes	table S3	yes		(**16a**) yes, (368 mg/L)	1
(17)	isopimaradiene	2005	yes		yes			1
(19)	*syn*-isopimaradiene-7,15-diene	2014	yes			yes, figure S10	yes	2
(18)	unknown	2020	no					3
(20a/b)	13*R*-*ent*-manoyl oxide/ 13S-(*+*)-manoyl oxide	2026	yes	table S3		yes, figure S11	(**20b**) yes, (329 mg/L)	1
(21)	kaur-16-ene	2055	yes					2
(22a/b)	(*+*)/*ent*-dehydroabietadiene	2062	yes		yes	yes, figure S9, S10	yes	1
(23a/b)	(*+*)/*ent*-manool	2065	yes	table S5	yes	yes, figure S2, S12	(**23a**) yes, (311 mg/L)	1
(24)	unknown	2072	yes					3
(25)	miltiradiene	2074	yes	table S7	yes	yes, figure S9	yes, 250 mg/L)	1
(26)	kolavelool	2074	yes	table S6		yes, figure S13		1
(27a/b)	(*+*)/*ent*-abietadiene	2091	yes		yes			1
(28)	unknown	2095	no					3
(29)	unknown	2098	no					3
(30a/b)	unknown	2115	yes					2
(31)	unknown	2120	no					3
(32)	unknown	2128	yes					3
(33)	unknown	2129	yes					3
(34a/b)	(*+*)/*ent*-neoabietadiene	2158	yes		yes			1
(35)	unknown	2167	no					3
(36a/b)	(*+*)/*ent*-abienol	2186	yes					2

(37)	unknown	2192	yes					3
(38)	unknown	2194	no					3
(39)	unknown	2199	no					3
(40)	unknown	2202	yes					3
(41)	unknown	2215	yes					3
(42)	unknown	2227	no			not formed in vitro, figure S7		3
(43a/b)	(+)/*ent*-sclareol	2230	yes		yes			1
(44)	unknown	2236	yes					3
(45)	kaur-16-anol	2244	yes					2
(46)	unknown	2246	yes					3
(47)	unknown	2268	no					3

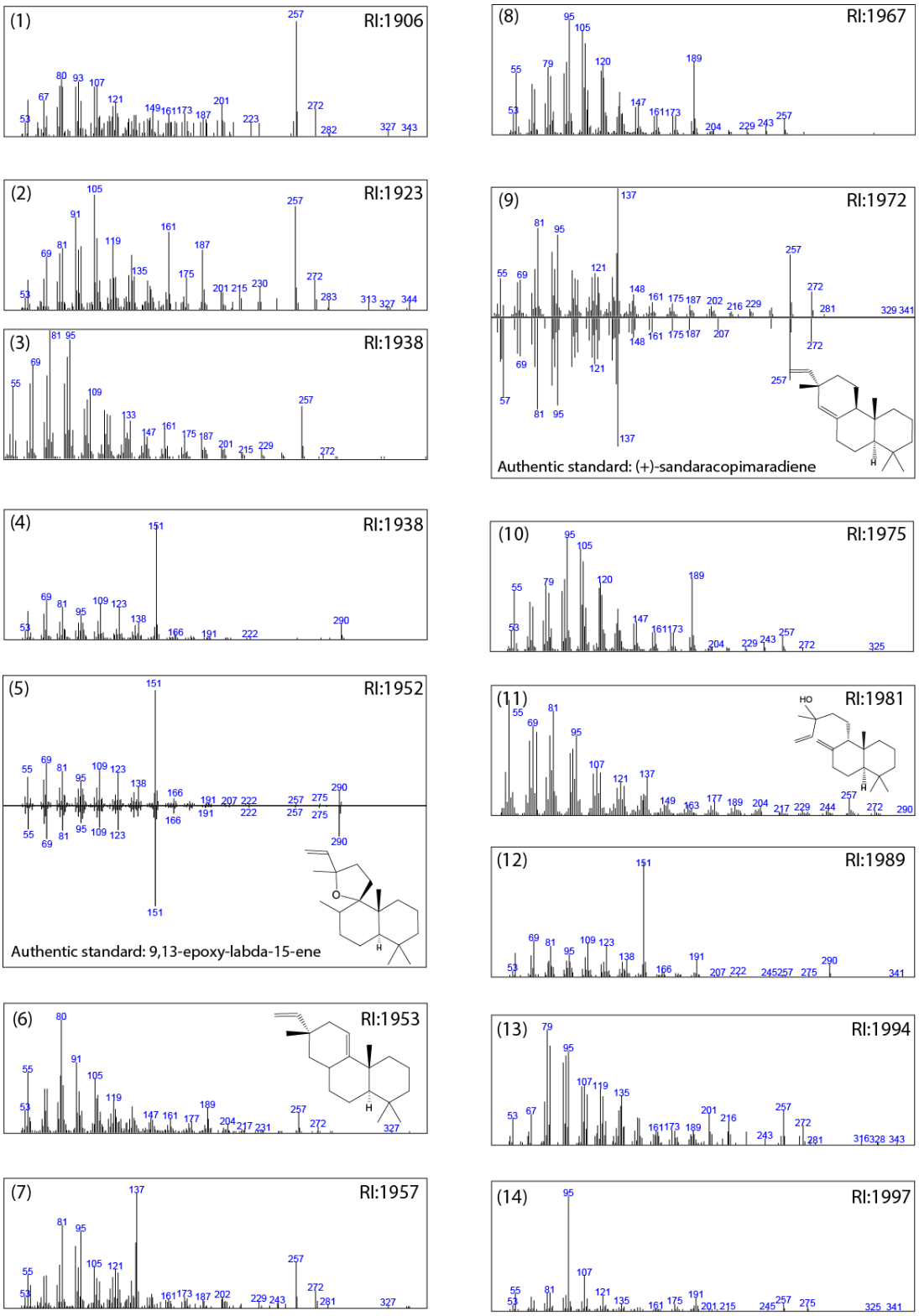

Supplementary figure S1. Mass spectra of compounds 1-14 identified in this work.

Reference MS spectra available are mirrored to the MS spectra obtained in this work. NMR analysis of *syn*-manool (**11**) and *syn*-pimara-9,(11),15-diene (**6**) can be found in supplementary table S5 and S8, respectively.

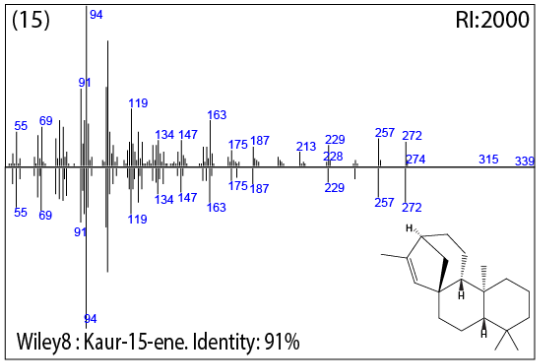

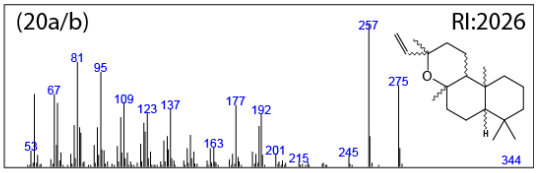

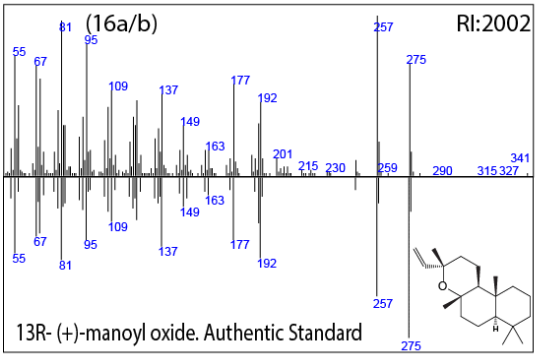

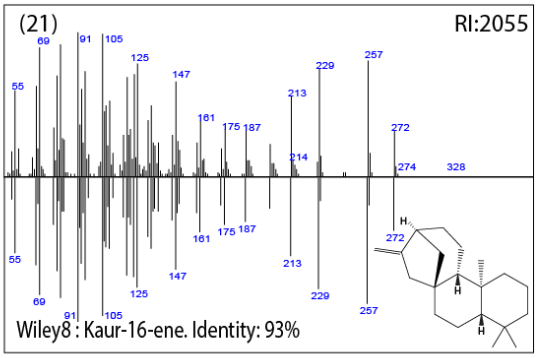

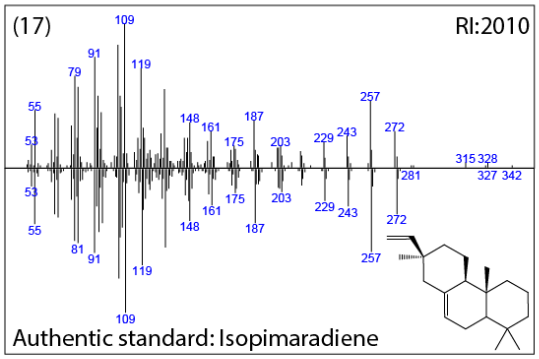

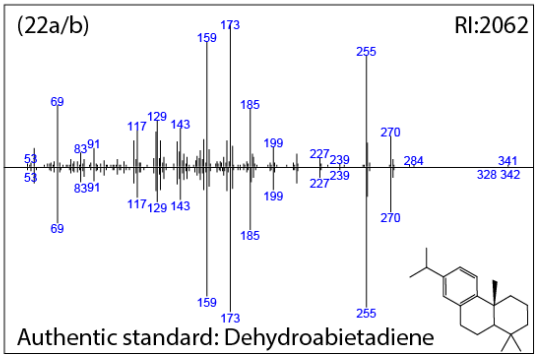

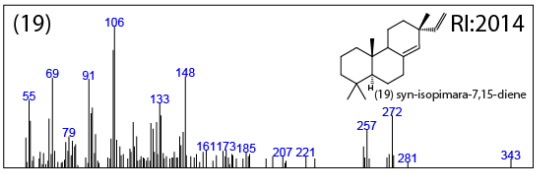

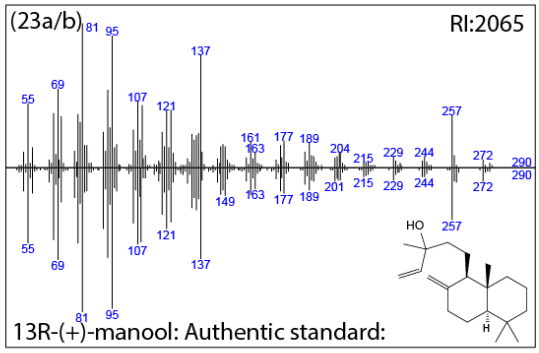

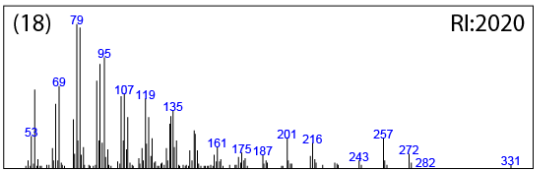

Supplementary figure S2. Mass spectra of compounds 15-23 identified in this work.

Reference MS spectra available are mirrored to the MS spectra obtained in this work. Syn-isopimara-7,15-diene (**19**) was identified as product from combinations with OssynCPS and identified by comparison to mass spectra obtained in work combining OssynCPS with TaKSL4 (Ta, *Triticum aestivum*).[9] NMR analysis of 13*R*-(+)-/*ent*-manoyl oxide (**16a/b**), 13*R*-*ent*-manoyl oxide (**20b**) and *ent*-/(+)-manool (**23a/b**) is given in supplementary table S3 and S5.

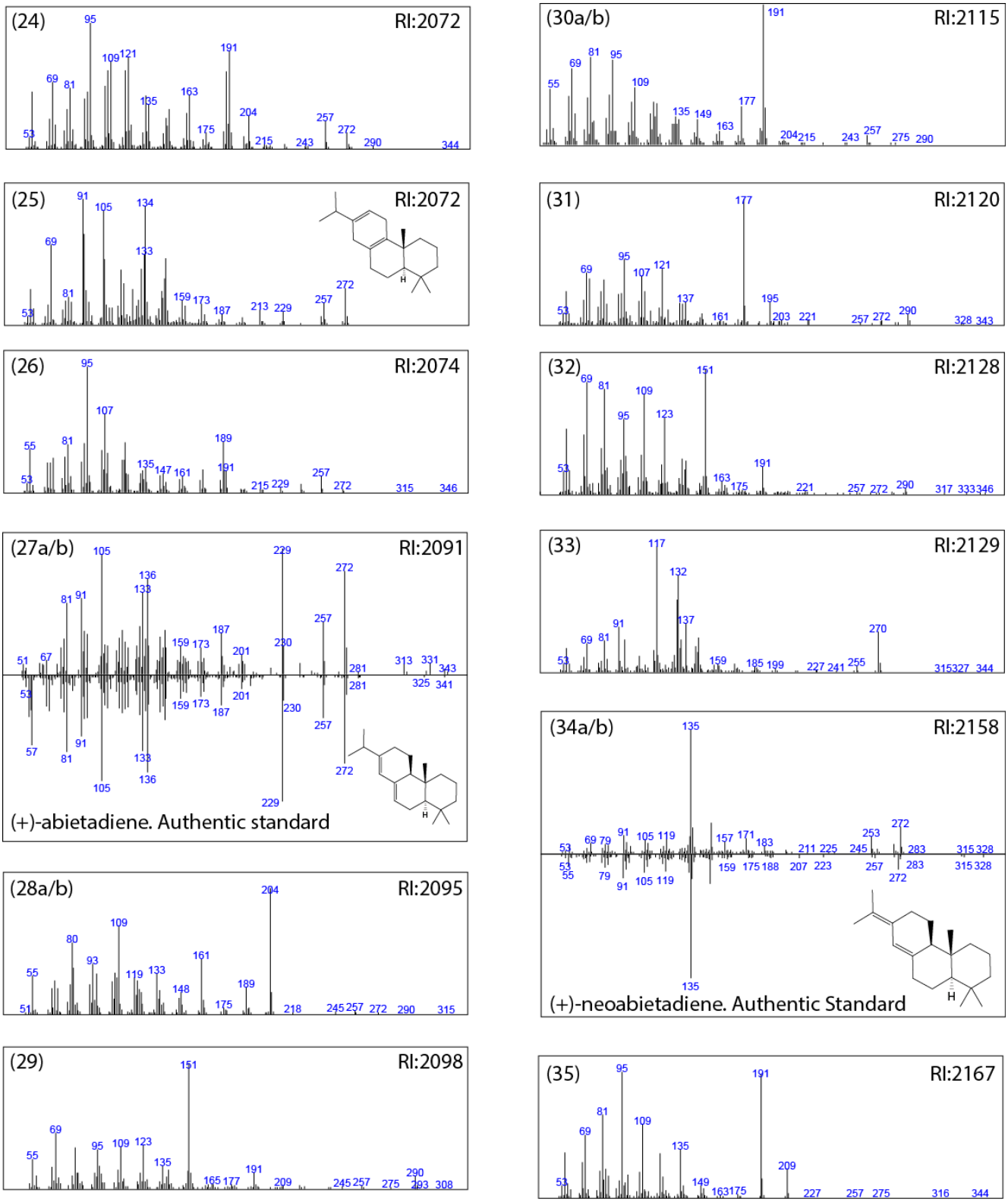

Supplementary figure S3. Mass spectra of compounds 24-35 identified in this work.

Reference MS spectra available are mirrored to the MS spectra obtained in this work. NMR analysis of miltiradiene (**25**) can be found in supplementary table S7.

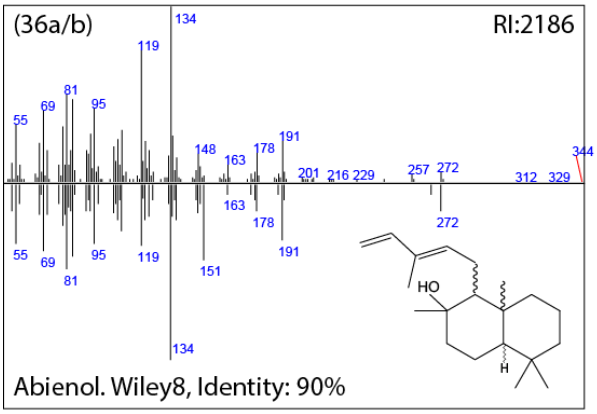

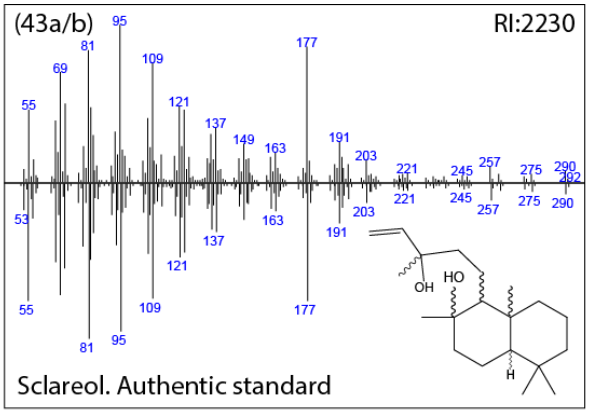

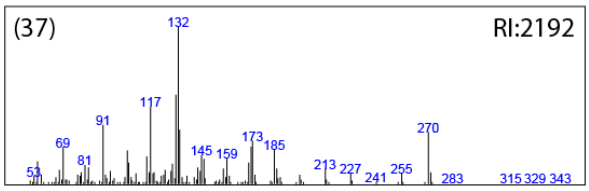

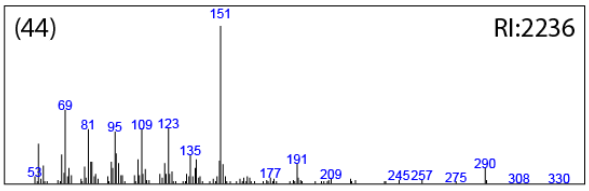

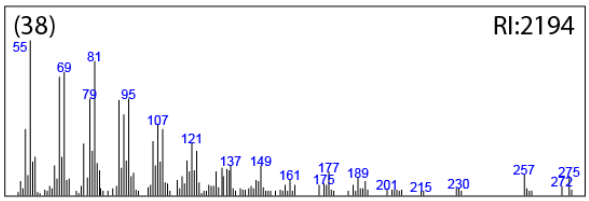

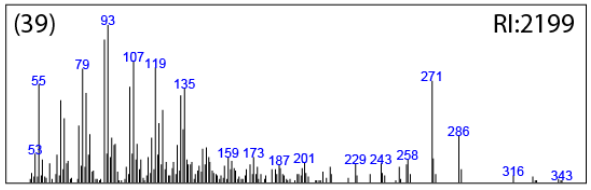

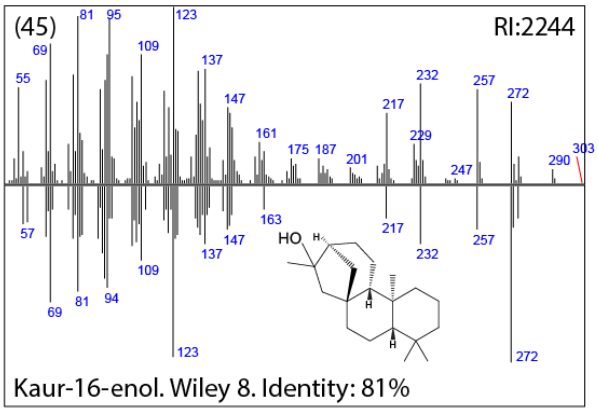

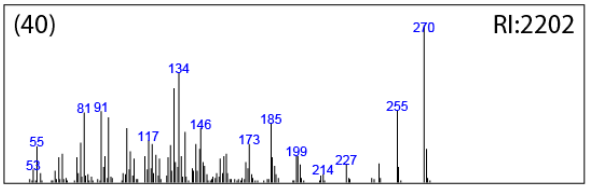

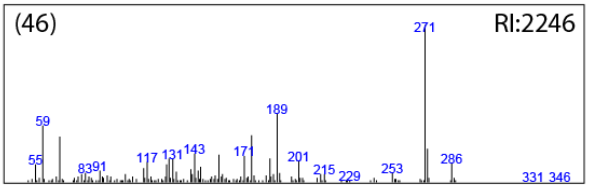

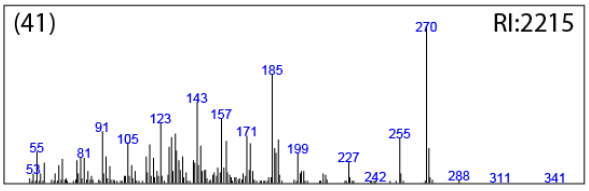

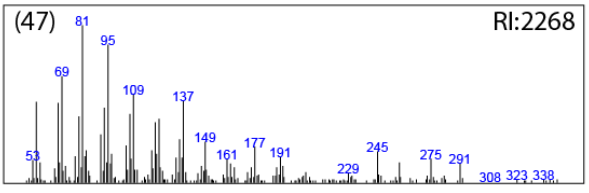

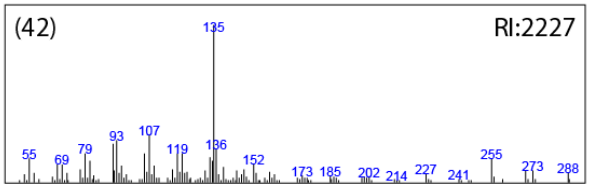

Supplementary figure S4. Mass spectra of compounds 36-47 identified in this work.

Reference MS spectra available are mirrored to the MS spectra obtained in this work.

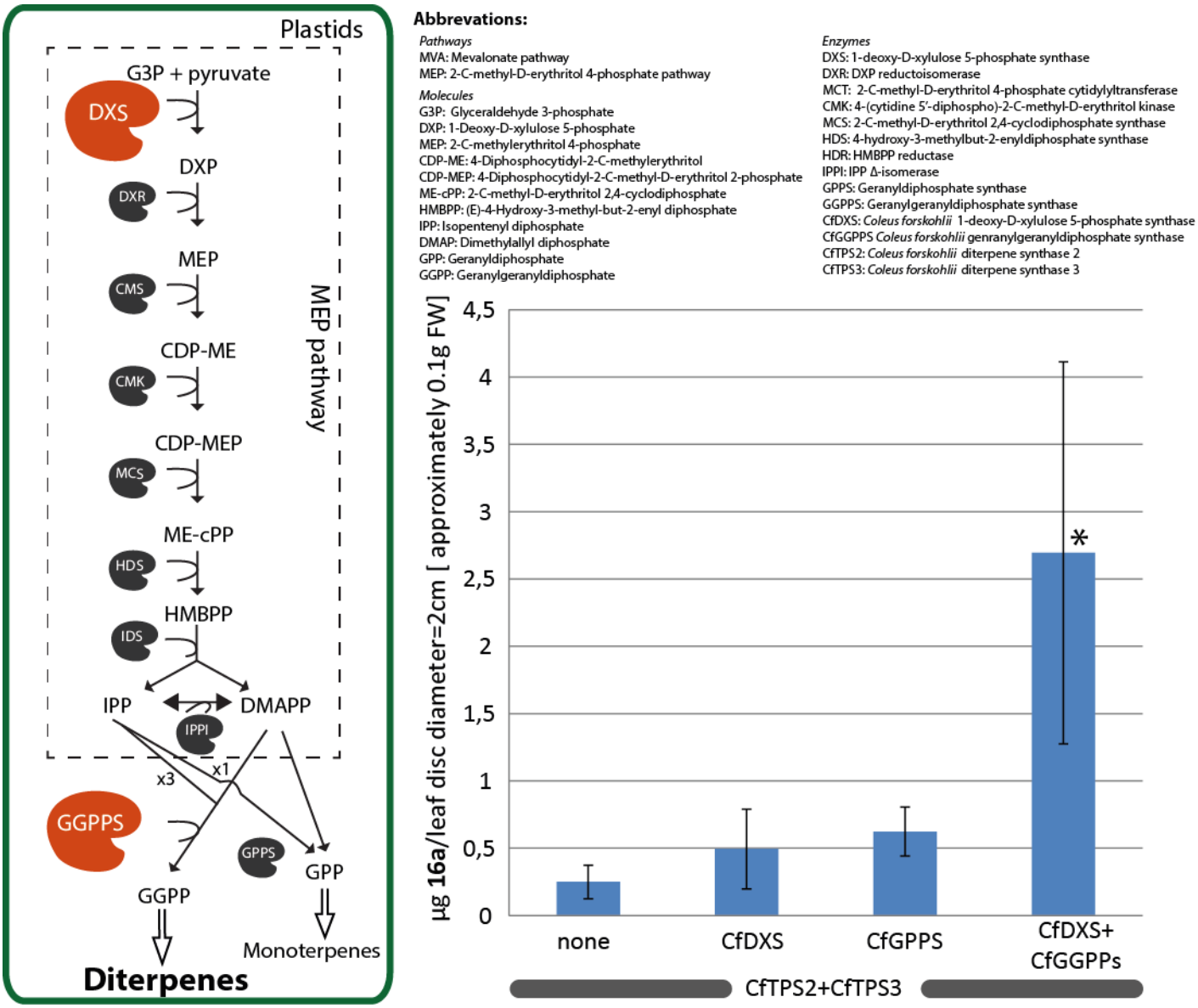

Supplementary figure S5. Biosynthetic yield of diterpenes from *N. benthamiana*.

Schematic overview of the MEP pathway (left). Quantification of 13*R*-(+)-manoyl oxide (**16a**) in hexane extracts from *N. benthamiana* leaf discs (2 cm diameter, corresponding to approximately 0.1 g fresh weight (FW)) transiently expressing CfTPS2/CfTPS3, CfTPS2/CfTPS3/CfDXS (CfDXS), CfTPS2/CfTPS3/CfGGPPS (CfGGPPS) and CfTPS2/CfTPS3/CfDXS/GGPPS (CfDXS+CfGGPPS) (Cf, *Coleus forskohlii*). **16a** was quantified in six biological replicates five days after infiltration. Error bars indicate standard deviation. An asterisk indicates statistical significant difference from the control (none) ($p<0.05$, Tukey's test). By transient co-expression of DXS2 from *Solanum lycopersicum* and GGPPS2 from *Nicotiana tabacum* together with diTPSs in *N. benthamiana* similar results have been reported earlier.[10] The approach enabled the purification of 0.5-5 mg of diterpenes for NMR structural analysis.

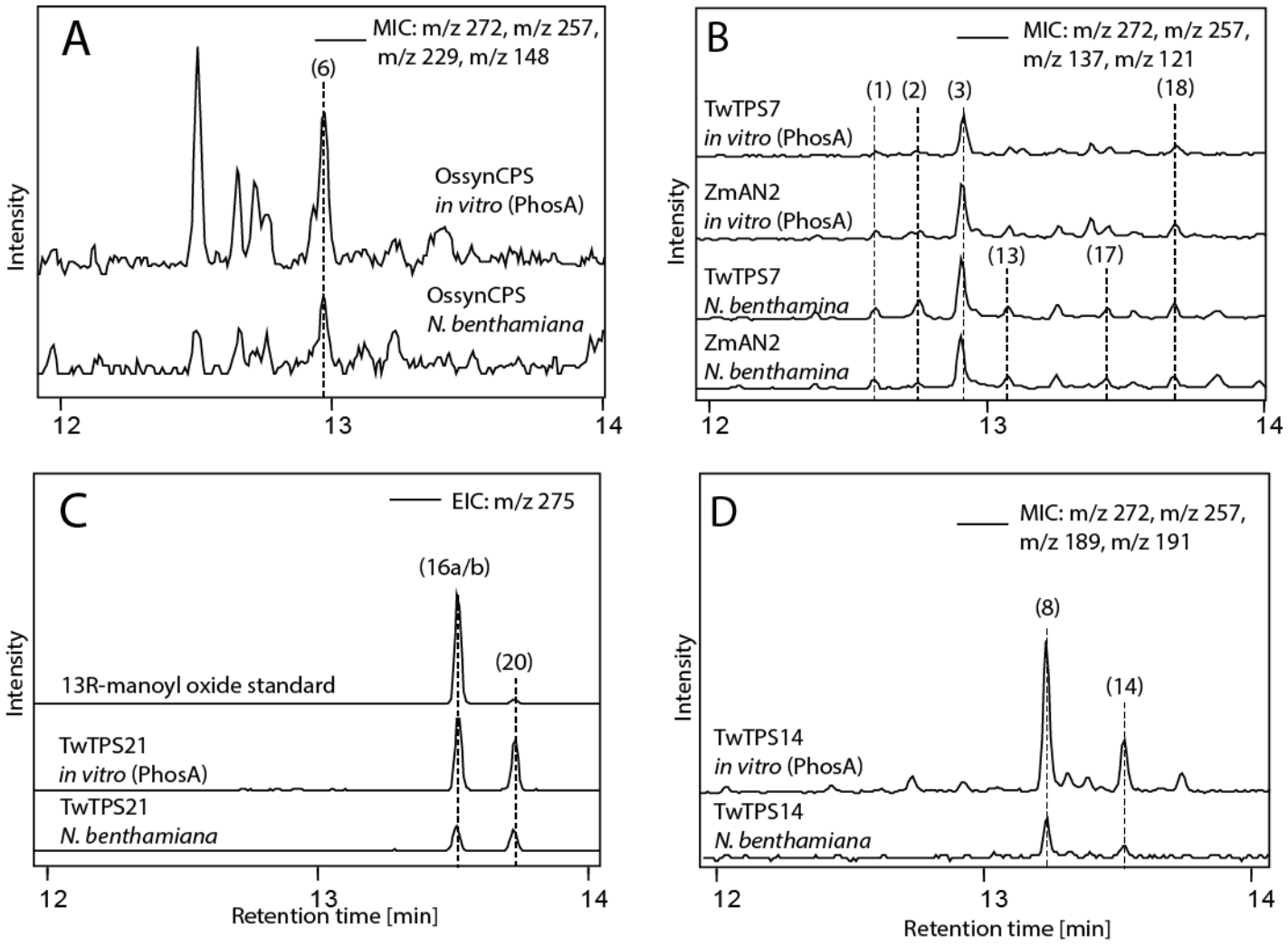

Supplementary figure S6. Comparison of class II diTPS products by GC-MS from transient expression in *N. benthamiana* and phosphatase treated metabolite extracts from *in vitro* assays.

Chromatograms show the mass ion chromatogram (MIC) representing characteristic ions for the compounds of interest.

A-D: Analysis of hexane extracts from phosphatase treated *in vitro* assays (PhosA) and of *N. benthamiana* extracts expressing OssynCPS, TwTPS7, ZmAN2, TwTPS21 and TwTPS14 (Os, *Oryza* sativa; Tw, *Tripterygium wilfordii*; Zm, *Zea mays*). The majority of the compounds in single class II diTPS assays detected *in planta* can indeed be derived from dephosphorylation of class II diTPS products from *in vitro* assays. This is in agreement with previous findings reported for CfTPS2 and MvCPS1.[1, 4]

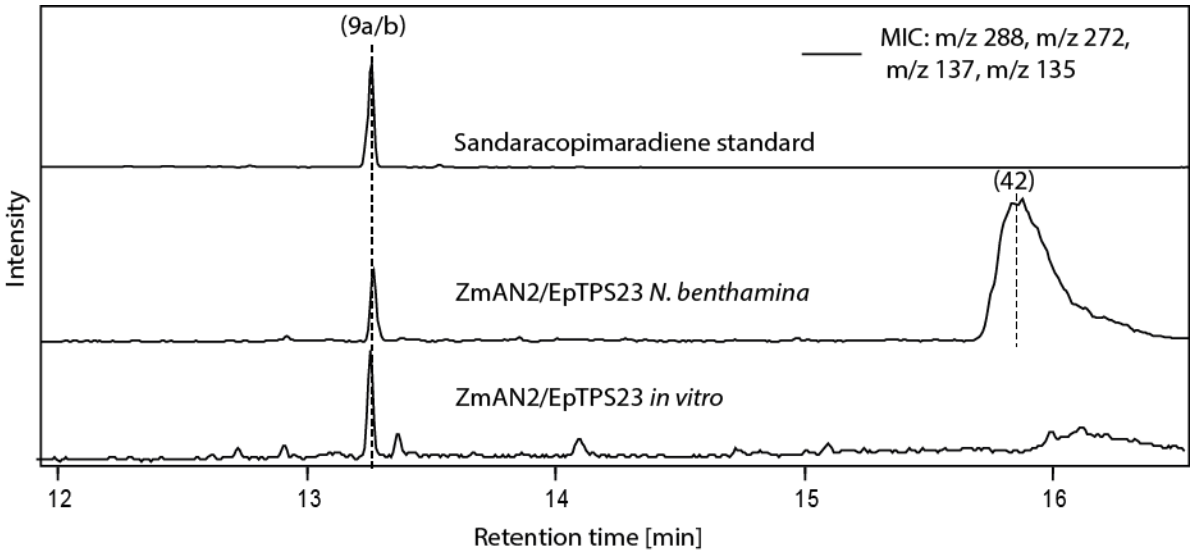

Supplementary figure S7. Hydroxylation of *ent*-sandaracopimaradiene by endogenous *N. benthamiana* enzymes.

Comparison of diterpene compounds detected by GS-MS in extracts from *in vitro* assays and from *N. benthamiana* expressing ZmAN2 and EpTPS8. Chromatograms show the MIC representing characteristic ions for the compounds of interest. Sandaracopimaradiene in a presumed *ent*-configuration (**9b**) was identified both in extracts from *N. benthamiana* and *in vitro* assays with ZmAN2/EpTPS23 (Zm, *Zea mays;* Ep, *Euphorbia peplus*). An unknown diterpene related compound with a mass of m/z 288 (**42**), characteristic of hydroxylated diterpenes,[11] was only identified in *N. benthamiana*, indicating possible nonspecific conversion of **9b** by endogenous *N. benthamiana* enzyme(s).

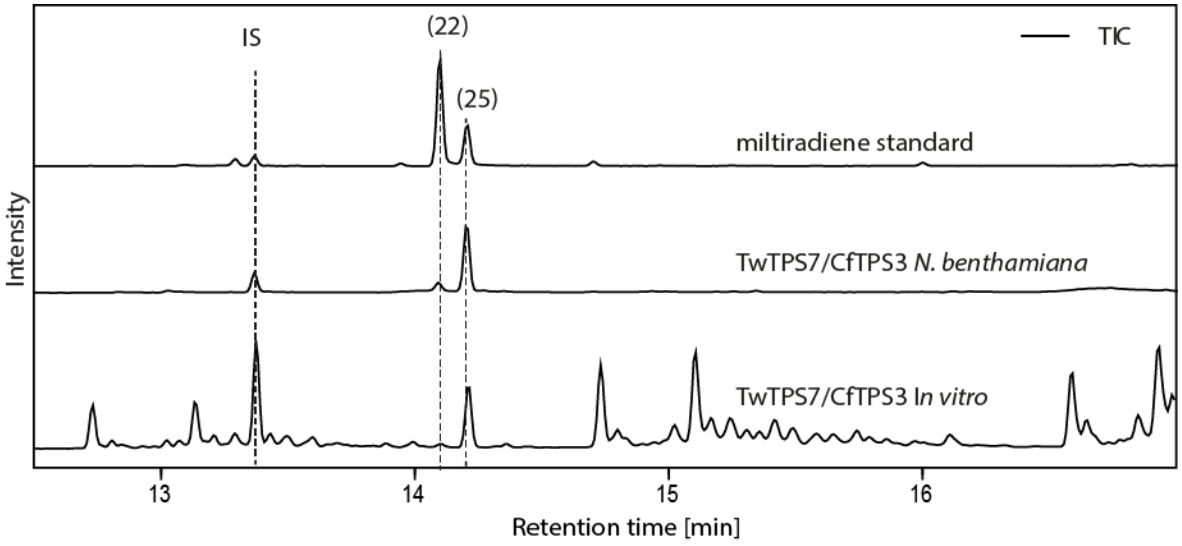

Supplementary figure S8. Comparison of products from *N. benthamiana* and *in vitro* assay extracts, utilizing the "new-to-nature" combination of TwTPS7/CfTPS3.

The chromatograms display the total ion chromatogram (TIC). The identity of **25** was established by comparison of retention time and mass spectra with a miltiradiene standard confirmed by NMR analysis (supplementary figure S7). Formation of **25** and dehydroabietadiene (**22**) were observed in both the *N. benthamiana* and *in vitro* extract from TwTPS7/CfTPS3. Spontaneous desaturation of miltiradiene to dehydroabietadiene has previously been reported.[12] (Tw, *Tripterygium wilfordii*; Cf, *Coleus forskohlii*).

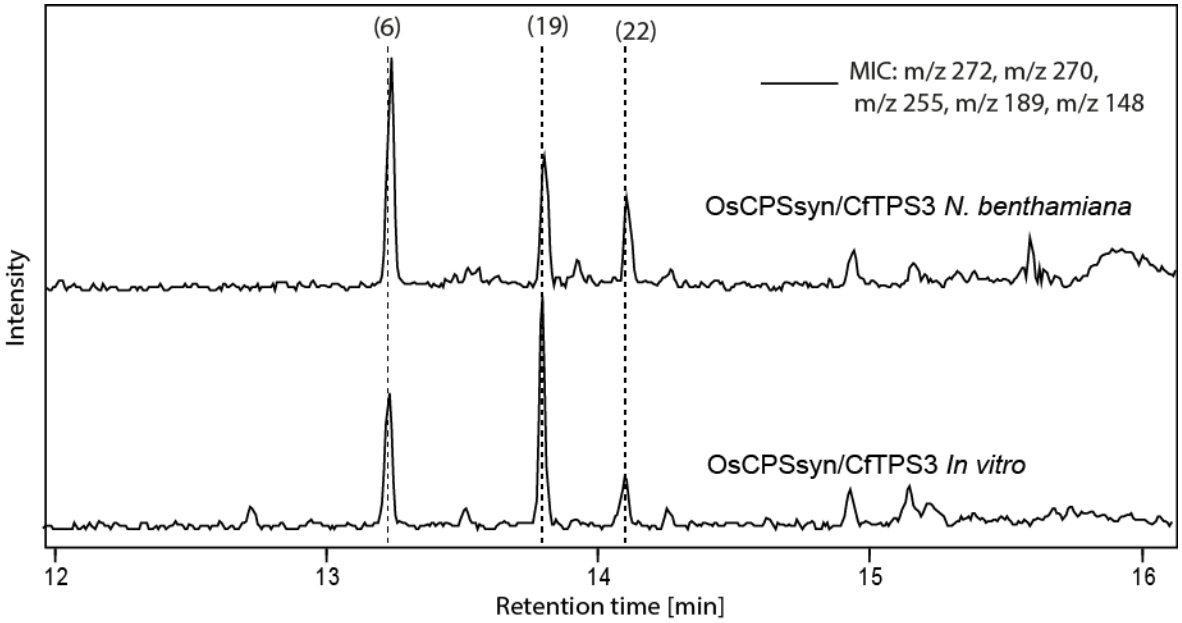

Supplementary figure S9. Comparison of products from *N. benthamiana* and *in vitro* assay extracts, utilizing the "new-to-nature" combination of OsCPSsyn/CfTPS3.

Chromatograms display the MIC representing characteristic ions for the compounds of interest. **6**, **19** and **22** were observed in both the *N. benthamiana* and *in vitro* extracts from OsCPSsyn/CfTPS3 (Os, *Oryza sativa*; Cf, *Coleus forskohlii*). **6** was established as *syn*-pimara-9(11),15-diene by NMR analysis (supplementary table S8).

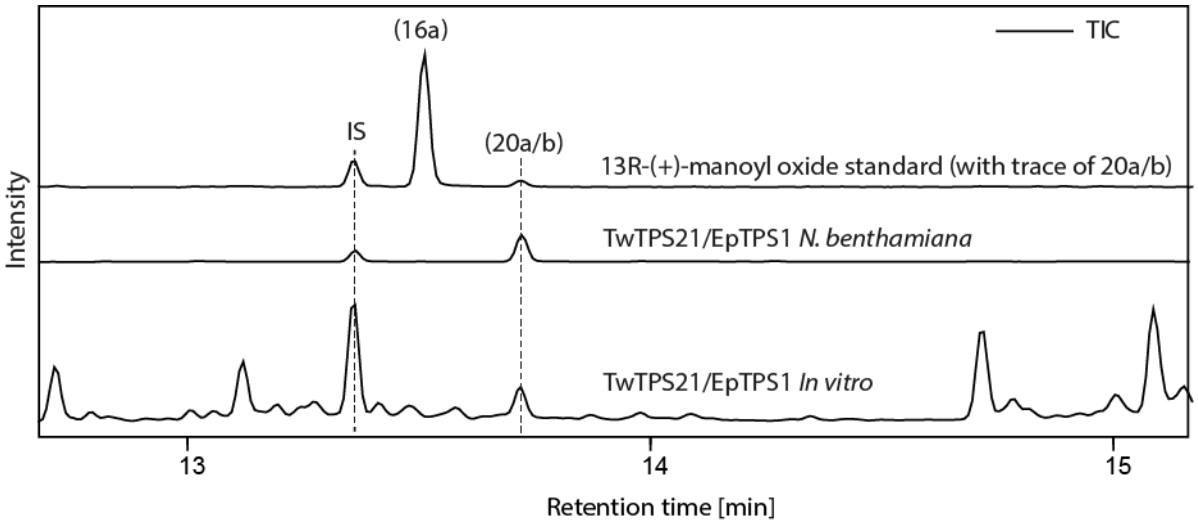

Supplementary figure S10. Comparison of products from *N. benthamiana* and *in vitro* assay extracts, utilizing the "new-to-nature" combination of TwTPS21/EpTPS1.

13*R*-*ent*-manoyl oxide (**20b**) was identified as the sole diterpene both in the *N. benthamiana* and *in vitro* assay extracts from the combination TwTPS21/EpTPS1 (Tw, *Tripterygium wilfordii*; Ep, *Euphorbia peplus*). The mass spectrum obtained from **20b** was similar to the mass spectrum of **16a**, and the retention time from the GC-MS analysis of **20b** on a HP5-MS column was significantly different from **16a**, and identical to trace amounts of **20a/b** identified in standard of **16a**. The identity of **20b** was established by NMR and optical rotation analysis (supplementary table S3 and S4). Biosynthesis of **20b** has previously been achieved in racemic mixture of manoyl oxides including **16a** and **20b** in *E. coli*, in which it was suggested to origin from inadequate coupling of class II and class I diTPS involved in biosynthesis of **16a.**[13] Furthermore biosynthesis of manoyl oxide isomers have been suggested as product of class I diTPS enzymatic rearrangement of (9*R*,10*R*)-labda-8-ol diphosphate (8-*ent*-LPP, figure 1) obtained from a mutated AtCPS from *Arabidopsis thaliana.*[14]

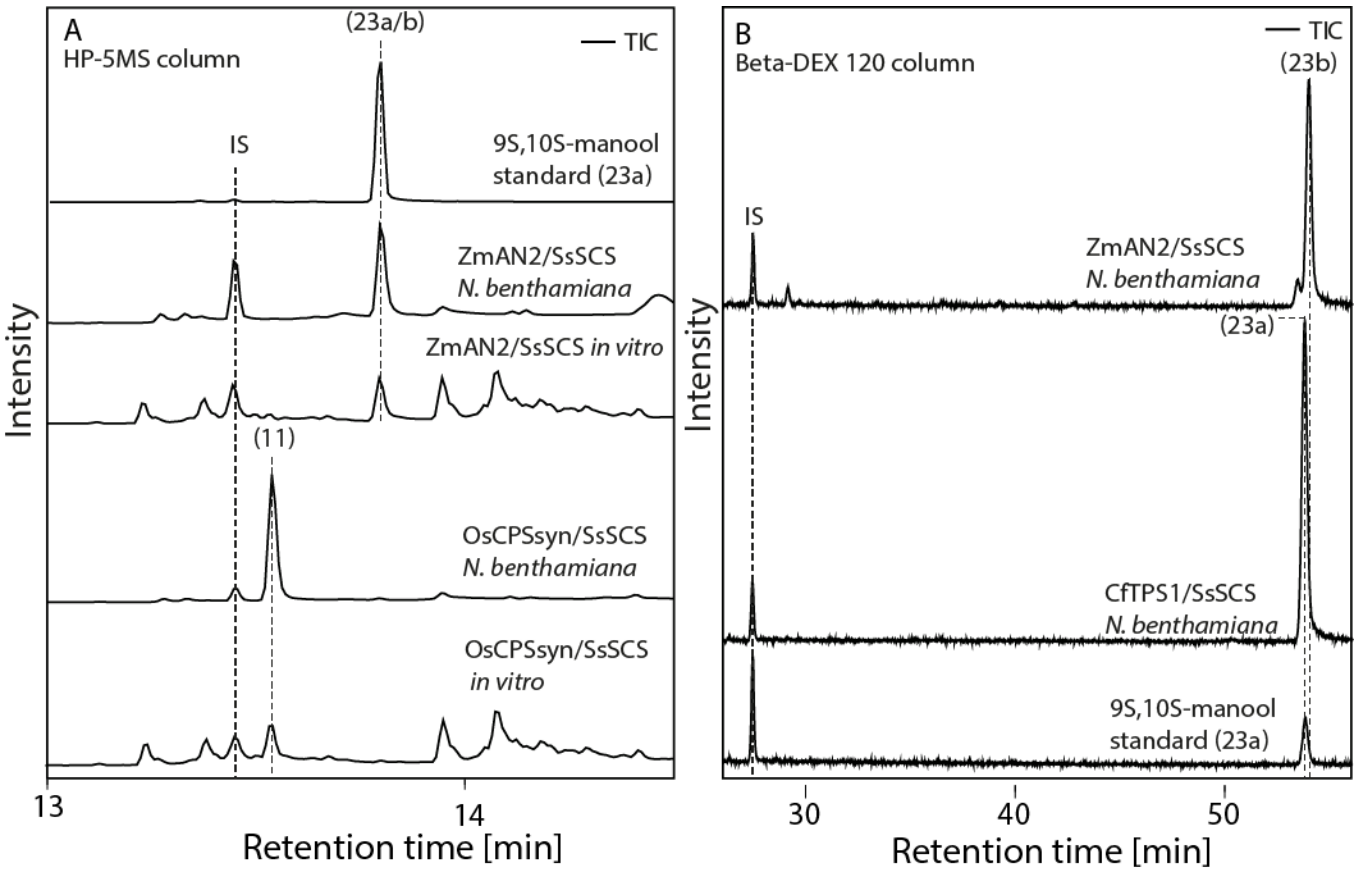

Supplementary figure S11. Comparison of products from *N. benthamiana* and *in vitro* assays, utilizing the "new-to-nature" combinations of ZmAN2/SsSCS and OsCPSsyn/SsSCS.

The GC-chromatograms are displayed as the total ion chromatogram (TIC).

A: *ent*-manool (**23b**) was identified both in the *N. benthamiana* and *in vitro* extracts from ZmAN2/SsSCS (Zm, *Zea mays*; Ss, *Salvia sclarea*). Retention time and MS spectra were identical to the authentic standard of (*+*)-manool (**23a**). Similarly *syn*-manool (**11**) was identified both in *N. benthamiana* and *in vitro* extracts from OsCPSsyn/SsSCS (Os, *Oryza sativa*; Ss, *Salvia sclarea*). Identities of **11** and **23b** were confirmed by NMR (supplementary table S5).

B: Separation of **23a** and **23b** by chiral GC. **23a** extracted from *N. benthamiana* expressing CfTPS1/SsSCS had an identical retention time to the authentic standard of 9*S*,10*S*-manool, whereas the retention time of **23b** from ZmAN2/SsSCS was significantly different from **23a**.

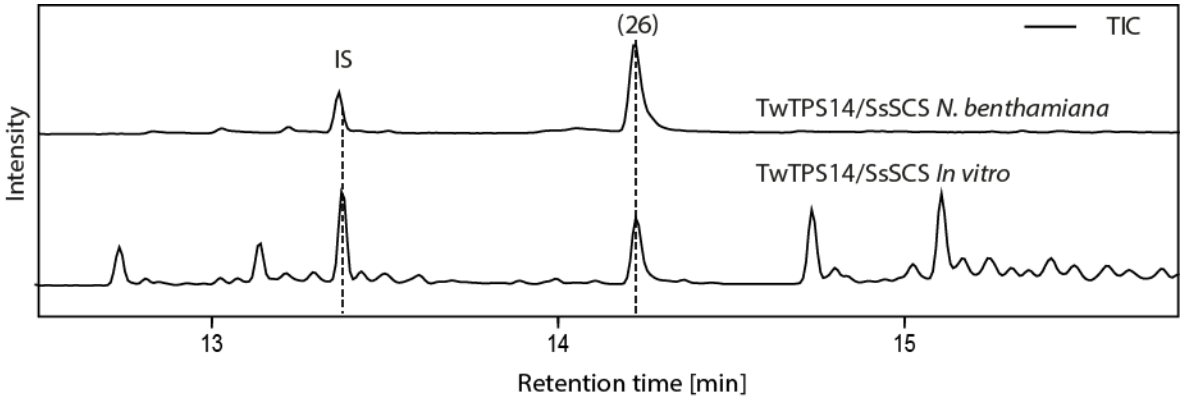

Supplementary figure S12. Comparison of products from *N. benthamiana* and in vitro assay extracts, utilizing the "new-to-nature" combination of TwTPS14/SsSCS.

Compound **26** was observed as the sole diterpene product in *N. benthamiana* and *in vitro* extracts from TwTPS14/SsSCS (Tw, *Tripterygium wilfordii*; SsSCS, *Salvia sclarea*). The identity of kolavelool (**26**) was confirmed by NMR (supplementary table S6).

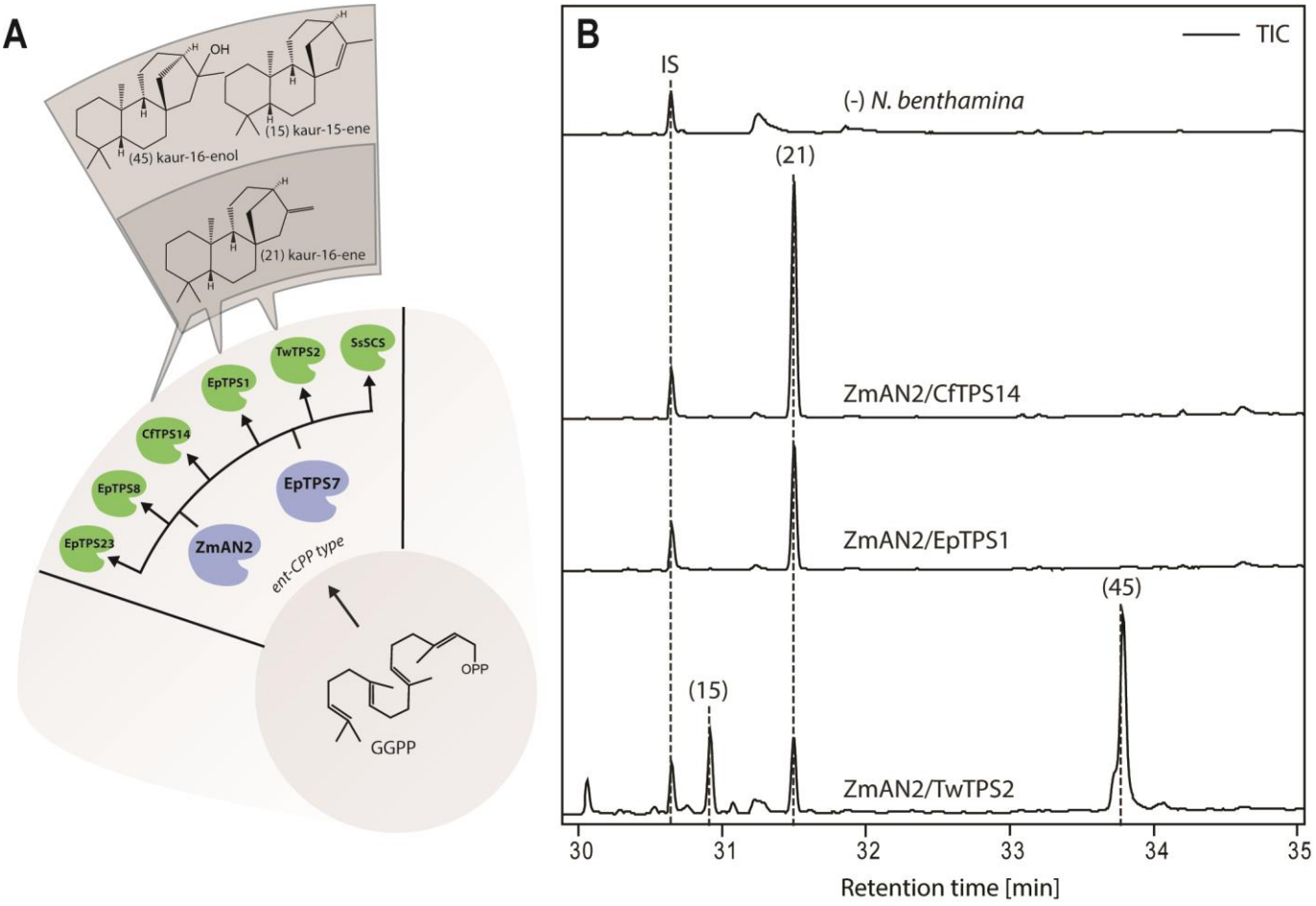

Supplementary figure S13. Biosynthesis of kaurene isoforms from CfTPS14, EpTPS1 and TwTPS2 in combination with *ent*-CPP type class II diTPSs.

A: Combinations of diTPSs resulting in the formation of kaurene isoforms from GGPP.

B: GC-MS analysis of hexane extracts from *N. benthamiana* expressing ZmAN2 in combination with CfTPS14, EpTPS1 or TwTPS2. Identification of *ent*-kaur-15-ene (**15)**, ent-kaur-16-ene (**21)**, and ent-kaur-16-enol (**45**) was based on comparison of MS spectra to library spectra (supplementary figure S3 and S5). ZmAN2 and EpTPS7 have previously been characterized as *ent*-CPP type class II diTPSs (figure 1)[2, 6] and their coupling in combinations with EpTPS1, CfTPS14 and TwTPS2 led to formation of the tetracyclic diterpene **21**, precursor of the ubiquitous plant phytohormones gibberellins. Intriguingly, the combination of *ent*-CPP type class II diTPSs with TwTPS2 led to the biosynthesis of **15** and **45** in addition to **21**. To our knowledge **15** and **45** have not been reported as biosynthetic products from the combination of class II and class I diTPSs, indicating that TwTPS2 may have the capacity to form kaurene isoforms relevant outside the biosynthesis of gibberellin phytohormones. Several kaurene-derived diterpene natural products such as the natural sweetener stevioside and the pharmacologically active compounds from Chinese medicinal plant *Isodon eriocalyx* are of industrial interest.[15] (Zm, *Zea mays*; Cf, *Coleus forskohlii*; Ep, *Euphorbia peplus*; Tw, *Tripterygium wilfordii*)

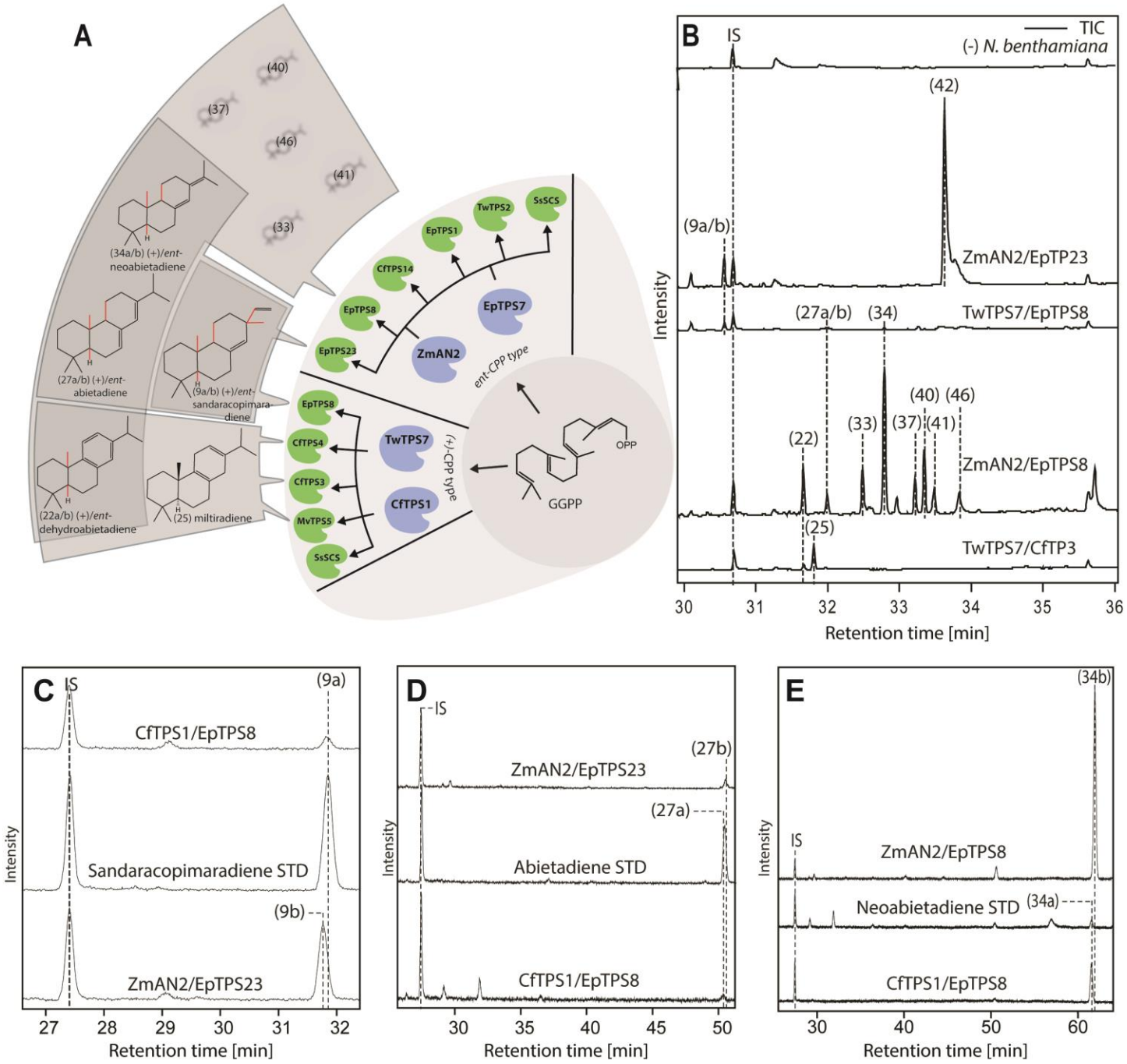

Supplementary figure S14. Biosynthesis of diterpene resin olefins stereoisomers from "new-to-nature" combinations of diTPSs.

A: Combinations of diTPSs resulting in the formation of diterpene resin olefin isomers from GGPP.

B: GC-MS analysis of hexane extracts from *N. benthamiana* expressing ZmAN2 or TwTPS7 together with EpTPS23 or EpTPS8, respectively. Identification of *ent*-/(+)-sandarcopimaradiene (**9a/b**), *ent*/(+)-abietadiene (**27a/b**), *ent*-/(+)-neoabietadiene (**34a/b**) and *ent*-/(+)-dehydroabietadiene (**22a/b**) was based on comparison to RI and MS spectra (supplementary figure S2 to S5) of authentic standards of **9a**, **27a**, **34a** and **22a**. Mass spectra of the identified

diterpenes **33**, **37**, **40**, **41** and **46**, are given in supplementary figures S4 and S5. *In vitro* assays support that **42** is not an enzymatic product from the combination of *ent*-CPP synthase type class II diTPSs and EpTPS23 but due to endogenous activity in *N. benthamiana* (supplementary figure S8).

C-E: GC-analysis of **9a** and **9b, 27a** and **27b, 34a** and **34b** on a chiral column. The identity of **9a**, **27a** and **34a** was confirmed by comparison to retention time and mass spectra of authentic standards. **9b**, **27b** and **34b** showed MS spectra similar to **9a**, **27a** and **34a** but significantly different retention times on the chiral column. This suggests that **9b**, **27b** and **34b** are stereoisomers of **9a**, **27a** and **34a**. Analysis of **34a/b** was performed in selected ion monitoring (SIM) mode, with ions m/z 272, 257, 148, 135, 125, specific for **34a/b** and the IS. EpTPS8 accepted both *ent*- and (*+*)-CPP as substrate, catalyzing the formation of distinct diterpene resin olefins, precursors for diterpene resin acids in conifers. In conifers, diterpene resin olefins occur specifically in (*+*)-configuration and are biosynthesized by the levopimaradiene/abietadiene synthase and the isopimaradiene synthase from GGPP and from (*+*)-copalyl diphosphate ((*+*)-CPP) by class I diTPS from *Pinus banksiana* and *Pinus contorta*.[16] With distinct stereochemical configurations defined by the class II diTPS, we suggest that EpTPS23 and EpTPS8 in combinations with either an *ent*-CPP or (*+*)-CPP synthase result in biosynthesis of sandarcopimaradiene, abietadiene, neoabitadiene and dehydroabietadiene in either an *ent*- or (*+*)-configuration. (Zm, *Zea mays*; Cf, *Coleus forskohlii*; Ep, *Euphorbia peplus*; Tw, *Tripterygium wilfordii*)

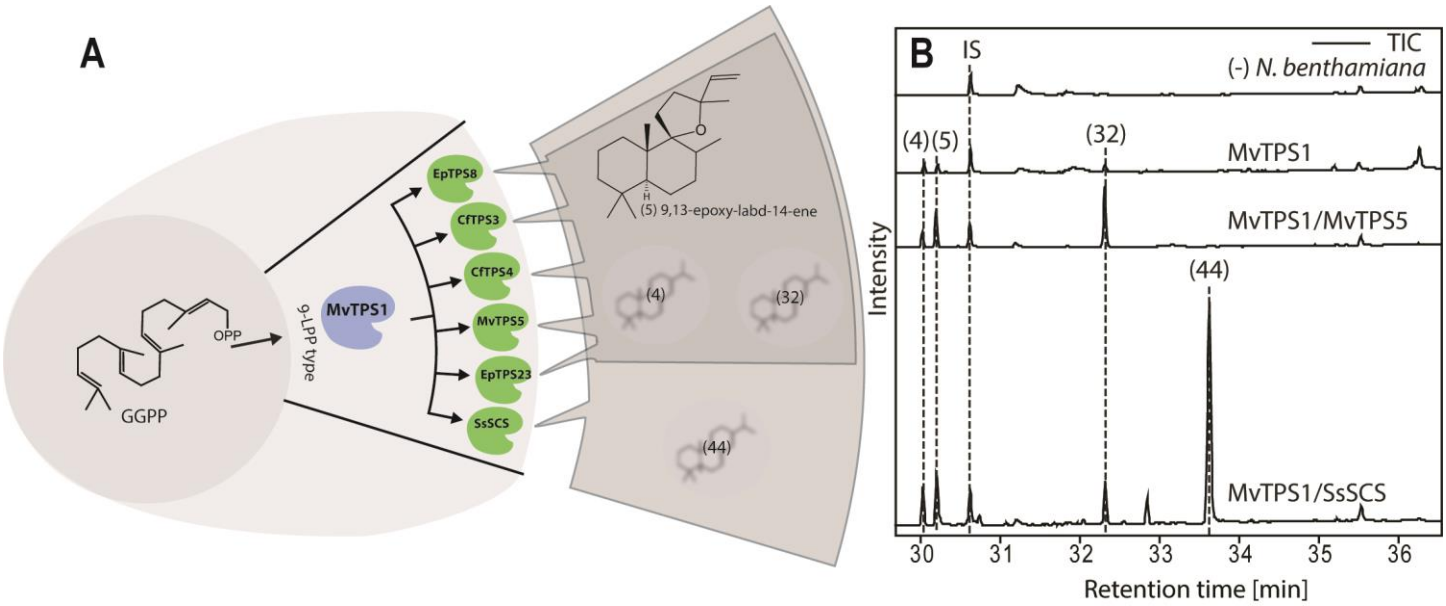

Supplementary figure S15. Biosynthesis of diterpenes from class I diTPSs in combinations with the MvCPS1.

A: Combinations of diTPSs resulting in the formation 9-LPP derived diterpene compounds.

B: GC-MS analysis of hexane extracts from *N. benthamiana* expressing MvCPS1 in combinations with MvELS or SsSCS. Compound **4**, 9,13-epoxy-labda-15-ene (**5**) and **32** were detected in the extracts from *N. benthamiana* expressing MvCPS1, MvCPS1/MvELS and MvCPS1/SsSCS. In the latter extract an additional unknown diterpene (**44**) was observed. Compounds **4**, **5**, **32** were identified by comparison of the retention time and MS spectra (supplementary figure S2 and S4) with previously described products from *N. benthamiana* expressing MvCPS1.[4] The native diTPS combination of MvCPS1 and MvELS facilitated biosynthesis of **5**, the putative biosynthetic precursor for marrubiin, a bioactive terpenoid with extensive therapeutic applications[4]. The new-to-nature combinations of MvCPS1 with CfTPS3 or CfTPS4 displayed a biosynthetic function similar to the natural diTPS combination suggesting alternative biosynthetic routes. In contrast, the diTPS combination of MvCPS1 and SsSCS resulted in the biosynthesis of predominantly **44**, with trace amounts of **5**, **4** and **32**. NMR analysis of **4** and **32** and **44** is required to establish the precise structure of these. Mv, *Marrubium vulgare*; Ss, *Salvia sclarea*.

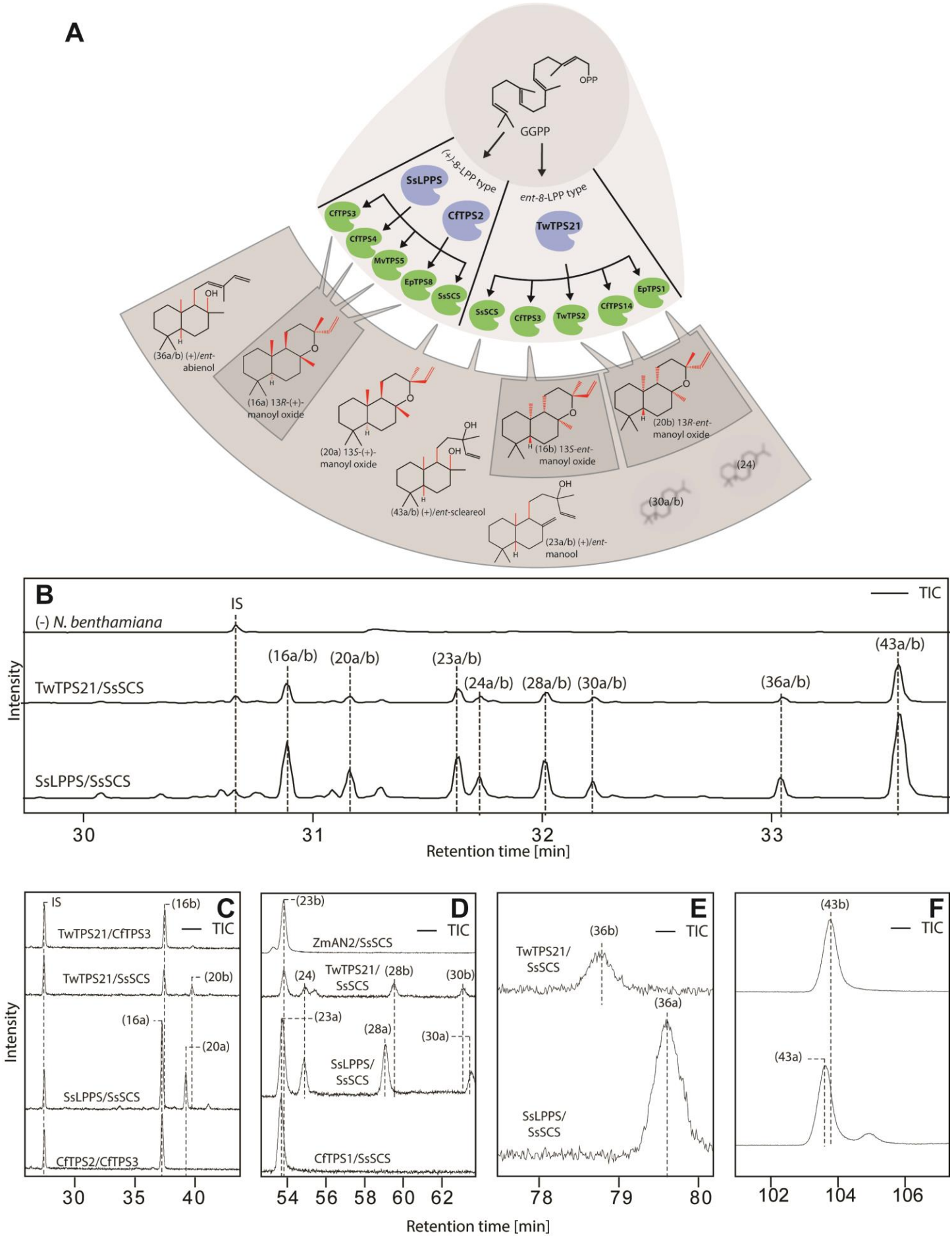
A
OPP
GGPP
(+)-8-LPP type
ent-8-LPP type
SsLPPS
CfTPS2
CfTPS3
CfTPS4
MvTPS5
EpTPS8
SsSCS
TwTPS21
SsSCS
CfTPS3
TwTPS2
CfTPS14
EpTPS1
OH
(36a/b) (+)/ent-abienol
(16a) 13R-(+)-manoyl oxide
(20a) 13S-(+)-manoyl oxide
(43a/b) (+)/ent-sclareol
(16b) 13S-ent-manoyl oxide
(20b) 13R-ent-manoyl oxide
(24)
(30a/b)
(23a/b) (+)/ent-manool
B
TIC
(-) N. benthamiana
IS
(16a/b)
(20a/b)
(23a/b)
(24a/b)
(28a/b)
(30a/b)
(36a/b)
(43a/b)
TwTPS21/SsSCS
SsLPPS/SsSCS
Intensity
30
31
32
33
Retention time [min]
C
IS
(16b)
TwTPS21/CfTPS3
TwTPS21/SsSCS
(20b)
(16a)
(20a)
SsLPPS/SsSCS
CfTPS2/CfTPS3
30
35
40
D
(23b)
ZmAN2/SsSCS
(24)
TwTPS21/ SsSCS
(28b)
(30b)
(23a)
(28a)
(30a)
SsLPPS/ SsSCS
CfTPS1/SsSCS
54
56
58
60
62
E
(36b)
TwTPS21/ SsSCS
(36a)
SsLPPS/ SsSCS
78
79
80
F
(43b)
(43a)
102
104
106
Retention time [min]

Supplementary figure S16. Biosynthesis of diterpenes from combinations with class II diTPSs catalyzing the formation of (*+*)-8-LPP and *ent*-8-LPP.

A: Combinations of diTPSs resulting in the formation (*+*)-8-LPP and *ent*-8-LPP derived diterpene compounds.

B: GC-MS analysis on a HP-5MS column of hexane extracts from *N. benthamiana* expressing TwTPS21 or SsLPPS in combinations with SsSCS. Compounds 13*R*-(*+*)-/13*S*-*ent*-manoyl-oxide **16a/b**, 13*S*-(*+*)-/13*R*-*ent*-manoyl-oxide **20a/b**, (*+*)-/*ent*-manool **23a/b**, diterpene **24a/b**, diterpene **28a/b**, diterpene **30a/b**, (*+*)-/*ent*-abienol 36a/b and (*+*)-/*ent*-sclareol **43a/b** were identified in the extracts from *N. benthamiana* expressing the pairs TwTPS21 and SsSCS, and SsLPPS and SsSCS. The compounds were identified by comparison of the retention index and MS spectra (supplementary table S2 and figures S3 to S5). **16a/b**, **20a/b**, **23a/b** and **43a/b** have previously been described as biosynthetic products from *in vitro* assays with SsLPPS and SsSCS.[3] **43a** is used as starting material for semisynthesis of the perfume constituent ambrox.[17]

C-F: GC-MS analysis on a chiral column (Supelco Beta DEX™ 120 (30 m x 0.25 mm i.d., 0.25 µm film thickness) of combinations TwTPS21/SsSCS, SsLPPS/SsSCS, TwTPS21/CfTPS3, CfTPS2/CfTPS3, ZmAN2/SsSCS and CfTPS1/SsSCS. C: **16b** was identified as product from the combinations TwTPS21/CfTPS3 and TwTPS21/SsSCS, whereas **16a** was identified in SsLPPS/SsSCS and SsLPPS/CfTPS3. **20a** and **20b** were identified from combinations of TwTPS21/SsSCS and SsLPPS/SsSCS, respectively. The identified structures of **16a**, **16b** and **20b** (supplementary table S3) and the significantly different retention times of **20a** and **20b** on the chiral column suggested that **20a** is the enantiomer of **20b**.

D: **23b** was identified as product from the combinations ZmAN2/SCS and the TwTPS21/SsSCS, whereas **23a** was identified both as products of the combination SsLPPS/SsSCS and CfTPS1/SsSCS. **28b** was identified from the TwTPS21/SsSCS combination and mass spectra were identical to **28a** identified as product from the SsLPPS/SsSCS combination. Because of the significantly different retention times of **28a** and **28b** on the chiral column, these are suggested to be stereoisomers. The stereochemical configuration of individual intermediates provided by TwTPS21 and SsLPPS, *ent*-8-LPP and (*+*)-8-LPP, is consistent with **28a** and **28b** in (*+*)- and *ent*-configuration, respectively. Analogously, **30a** and **30b** are given in (*+*)- and *ent*-configuration, respectively. Compound **24** was detected from both the combinations TwTPS21/SsSCS and SsLPPS/SsSCS. The distinct stereochemical configuration of the possible pair of **24** stereoisomers was not determined.

E-F: Compounds **36b** and **43b** were identified as product from the combination TwTPS21/SsSCS, whereas **36a** and **43a** were identified as product from the combination SsLPPS/SsSCS. The specific biosynthetic module and the significantly different retention times (n=3) of **36** and **43** in chiral GC analyses indicate that these compounds are pairs of stereoisomers in (*+*)- and *ent*-configuration.

Identification of diterpene structures and stereochemistry

Supplementary table S3: NMR data of manoyl oxide stereoisomers (16a), (16b) and (20b) recorded in chloroform-d_1

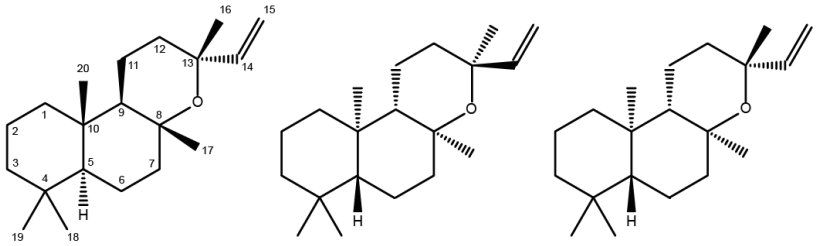

(16a) 13R-(+)-manoyl oxide (16b) 13S-*ent*-manoyl oxide (20b) 13R-*ent*-manoyl oxide

Position	13*R*-(*+*)-MO (**16a**) 13*S*-*ent*-MO (**16b**)[a,c]		13*R*-*ent*-MO (**20b**)[c]	
	δ_C	δ_H (*J* in Hz)	δ_C[b]	δ_H (*J* in Hz)
1	39.1	0.83, m 1.57, m	39.5	0.86, m 1.63, m
2	18.7	1.41, m 1.59, m	18.8	1.44, m 1.61, m
3	42.2	1.13. td (13.2, 4.3) 1.36, m	42.3	1.15, m 1.37, m
4	33.4		33.5	
5	56.6	0.93, dd (12.5, 2.4)	56.6	0.95, dd (12.3, 2.4)
6	20.1	1.27, m 1.65, m	20.1	1.27, m 1.65, m
7	43.4	1.45, m 1.82, dt (12.3, 3.3)	43.3	1.38, m 1.77, dt (12.1, 3.3)
8	75.2		76.3	
9	55.8	1.34, dd (11.9, 4.2)	58.6	1.21, m
10	37.1		37.0	
11	15.4	1.47, m 1.56, m	16.0	1.46, m 1.51, m
12	35.8	1.62, m 1.76, dt (13.3, 5.6)	35.0	1.46, m 2.21, m
13	73.3		73.4	
14	148.1	5.87, dd (17.5, 10.8)	147.9	6.01, dd (17.9, 11.0)
15	110.4	4.91, dd (10.8, 1.5) 5.14, dd (17.5, 1.5)	109.7	4.91, dd (11.0, 0.8) 4.97, dd (17.9, 0.8)
16	28.7	1.27, s	32.9	1.13, s
17	25.6	1.29, s	24.1	1.22, s
18	33.5	0.85, s	33.5	0.85, s
19	21.5	0.79, s	21.4	0.78, s
20	15.5	0.78, s	16.0	0.72, s

[a]The ^{1}H NMR of **16b** is identical to that of **16a**.[b] ^{13}C chemical shifts from one- and multiple-bond proton-detected 2D heteronuclear experiments. [c] acquired in HPLC-HRMS-SPE-NMR mode. The ^{13}C chemical shift of 16a and 16b matched

earlier reported data.[18] ^{1}H chemical shifts of H-14, H-15 (cis) and H-15 (trans) determining the stereochemistry of C-13 were consistent with values described in literature.[19]

Supplementary table S4: Optical rotation of manoyl oxides.

Compound	Optical rotation	Reference value
13*R*-(*+*)-manoyl oxide (**16a**)	$[\alpha]_D^{23}$ + 19 (*c* 0.7, $CHCl_3$)	$[\alpha]_D^{26}$ + 22 (*c* 0.1, $CHCl_3$) [20]
13*S*-*ent*-manoyl oxide (**16b**)	$[\alpha]_D^{23}$ – 48 (*c* 0.04, $CHCl_3$)[a]	
13*R*-*ent*-manoyl oxide (**20b**)	$[\alpha]_D^{23}$ – 50 (*c* 0.2, $CHCl_3$)	
(*+*)-manool (**23a**)	$[\alpha]_D^{24}$ + 24 (*c* 0.4, $CHCl_3$)	$[\alpha]_D^{24}$ + 26.9 (*c* 0.05, $CHCl_3$) [21]

[a] The limited amounts of **16b** resulted in uncertainty of the specific degree of rotation. However, the clear negative rotation together with NMR and GC-analyses on the chiral column confirm an enantiomeric relationship with **16a**.

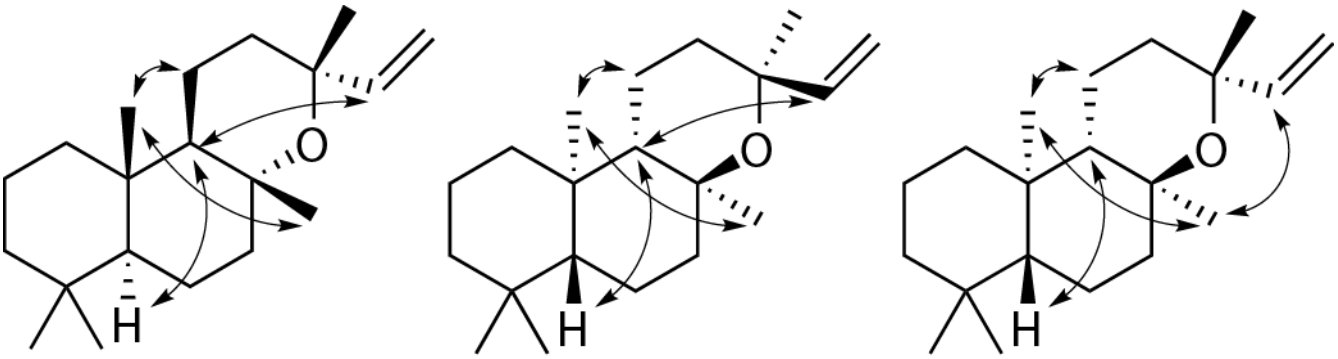

(16a) 13R-(+)-manoyl oxide (16b) 13S-*ent*-manoyl oxide (20b) 13R-*ent*-manoyl oxide

Supplementary figure S17. Key NOE correlations for assigning relative stereochemistry of manoyl oxide stereoisomers.

NMR analyses and GC-MS identified 13*R*-(*+*)-manoyl oxide (**16a**) and 13*S*-*ent*-manoyl oxide (**16b**) as having identical relative stereochemistry. **16a** and **16b** were separable by chiral GC (supplementary figure S17), thus identifying these as an enantiomeric pair. As **16a** has previously been investigated, comparison of optical rotation with those reported in the literature (table S4) identified the absolute stereochemistry of **16a**, and thus also of **16b**. Chemical shifts of H-14 and H-15a/b were in accordance with literature,[22] identified **20b** as a C-13 epimer of either **16a** or **16b**. As **20b** is produced through the same enzymatic pathway as **16b** an absolute stereochemistry of 13*S*-*ent*-manoyl oxide was established.

Supplementary table S5: NMR data of (*+*)-manool (23a), *ent*-manool (23b), and *syn*-manool (11) recorded in chloroform-d_1

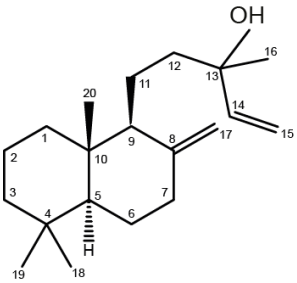

(23a) (+)-manool

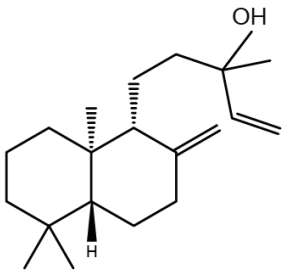

(23b) *ent*-manool

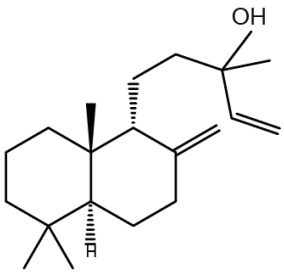

(11) *syn*-manool

Position	(*+*)-manool (**23a**) *ent*-manool (**23b**)[a,c]		*syn*-manool (**11**)[c]	
	δ_C	δ_H (*J* in Hz)	δ_C[b]	δ_H (*J* in Hz)
1	39.2	1.02 td (13.0, 4.3) 1.77 dt (13.0, 3.6)	36.9	1.04, ddd (12.5, 4.8, 2.8) 1.55, m
2	19.5		20.1	1.34, m 1.59, m
3	42.3	1.17, td (13.2, 3.8) 1.38 dt (13.2, 3.4)	42.7	1.17, td (13.4, 3.3) 1.39, m
4	33.7		32.9	
5	55.7	1.08, dd (12.6, 2.6)	45.8	1.32, m
6	24.6	1.47, m 1.56, m	23.8	1.30, m 1.63, m
7	38.5	1.93, td (13.0, 5.0) 2.37 ddd (12.6, 3.9, 2.1)	31.8	2.03, m 2.15, m
8	148.9		149.3	
9	57.4	1.56, m	58.5	1.48, m
10	40.0		37.4	
11	17.8	1.31, m 1.56, m	19.2	1.43, m 1.62, m
12	41.5	1.31, m 1.70, m	42.2	1.24, m 1.45, m
13	73.8		73.3	
14	145.3	5.94, dd (17.3, 10.8)	145.3	5.90, dd (17.3, 10.8)
15	111.8	5.06, d (10.8) 5.21, d (17.3)	111.6	5.05, dd (10.8, 0.7) 5.20, dd (17.3, 0.7)
16	28.2	1.27, s	28	1.27, s
17	106.5	4.48, s 4.80, s	109.5	4.49, bs 4.67, bs
18	33.8	0.87, s	33.6	0.87, s
19	21.9	0.80, s	22.3	0.80, s
20	14.6	0.67, s	22.5	0.91, s

The ^{1}H NMR of **23b** is identical to that of **23a**. [b] ^{13}C chemical shifts from one- and multiple-bond proton-detected 2D heteronuclear experiments. [c] acquired in HPLC-HRMS-SPE-NMR mode. **23a**, **23b**, and **11** were all analyzed as C-13 epimers with the 13*R* epimer being the dominant as reported earlier.[21] Relative stereochemistry determined through NOE correlations.

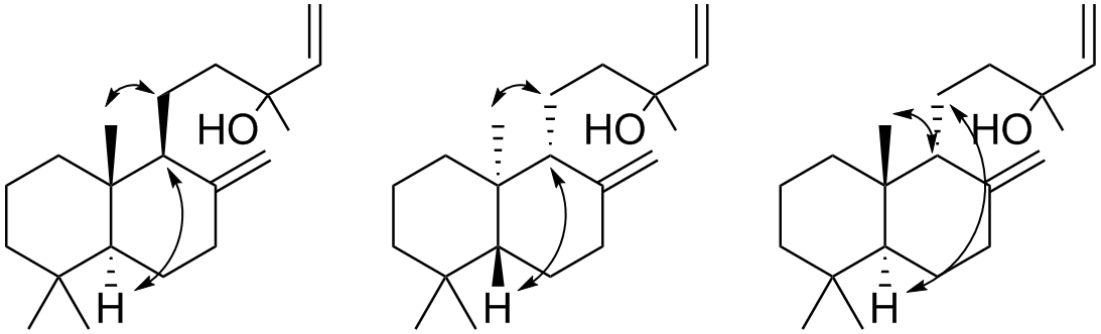

(**23a**) (+)-manool (**23b**) *ent*-manool (**11**) *syn*-manool

Supplementary figure S18. Key NOE correlations used for assigning relative stereochemistry of manool stereoisomers.

Relative stereochemistry of (*+*)-manool (**23a**), *ent*-manool (**23b**), and *syn*-manool (**11**) was established by key NOE correlations as shown. As **23a** and **23b** were separated on the chiral GC column (supplementary figures S12B) an enantiomeric relationship was confirmed and by measuring optical rotation of **23a** (supplementary table S4), absolute stereochemistry was established. NMR analyses identified *syn*-manool (**11**) as a C-9 epimer of either **23a** or **23b**. **11** was biosynthesized by the combination OssynCPS/SsSCS. As OssynCPS dictates the formation of *syn*-CPP with C-9 (*S*) and C-10 (*R*) configuration,[5] the absolute stereochemistry could be determined.

Supplementary table S6: NMR data of (*+*)-kolavelool (26) acquired in chloroform-d_1 in HPLC-HRMS-SPE-NMR mode.

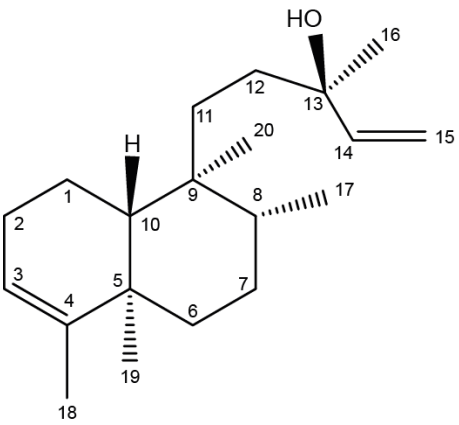

position	*[23]*		kolavelool (**26**)[c]	
	δ_C	δ_H (*J* in Hz)	δ_C[b]	δ_H (*J* in Hz)
1	18.2		18.2	1.41[a] 1.53[a]
2	27.4		27.0	2.01[a]
3	120.4	5.16 s	120.5	5.17, s
4	144.5		144.6	
5	38.1		37.4	
6	36.8		37.1	1.15[a] 1.69, dt (12.0, 3.0)
7	26.8		27.6	1.40[a]
8	36.1		36.3	1.41[a]
9	38.3		38.0	
10	46.3		46.5	1.3[a]
11	31.8		31.8	1.38[a] 1.25[a]
12	35.3		35.4	1.37[a]
13	73.4		73.2	
14	145.1	5.84 dd (17.2, 10.8)	145.2	5.87, dd (17.4, 10.7)
15	111.8	5.07 dd (17.2, 1.5) 4.99 dd (10.8, 1.5)	111.9	5.04, bd (10.7) 5.18, bd(17.4)
16	27.7	1.24 s	27.9	1.25, s
17	15.9	0.75 d (5.9)	16.0	0.76, d (5.7)
18	18	1.54 d (1.5)	18.0	1.57, bs
19	19.2	0.95 s	20.1	0.97, s
20	18.4	0.68 s	18.5	0.71, s

[a]Coupling constants not determined due to overlap with HOD; ^{1}H chemical shifts from HSQC experiments. [b] ^{13}C chemical shifts from one- and multiple-bond proton-detected 2D heteronuclear experiments. Relative stereochemistry determined through NOE correlations. **26** was identified as C-13 (*R*) epimer.

Supplementary table S7: Identification of miltiradiene (25).

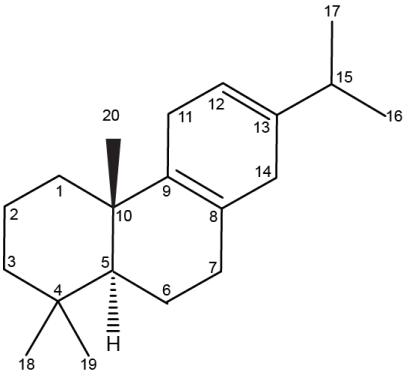

Position	(Gao, Hillwig et al. 2009)		This work	
	δ_C	δ_H (*J* in Hz)	δ_C [b]	δ_H (*J* in Hz)
1	37.0	1,68, m	36.9	1.72, m
2	19.3	1,44, m 1,57, m	19.2	1.40, m 1.60, m
3	42.0	1,13, m 1,39, m	42.0	1.11, td (12.9, 3.9) 1.15, td (13.6, 4.0)
4	33.3		33.4	
5	51.8	1,20, m	51.8	1.20, dd (12.7,2.0)
6	19.1	1,48, m 1,70, m	19.0	1.51, m 1.72, m
7	32.1	1,90, d 1,93, d	32.1	1.93, dd (17.2, 6.5) 2.01, m
8	124.3		124.1	
9	136.0		135.5	
10	37.4		37.3	
11	33.6	2,40, t 2,48, d	33.5	2.39, dt (20.9, 7.1) 2.51, dt (20.9, 7.6)
12	116.7	5,43, d	116.6	5.45, s
13	140.2		140.1	
14	25.7	2,61, s	25.6	2.63, s
15	34.4	2,16, m	34.4	2.19, sept (6.9)
16	21.4	0,99, d (2.5)	21.3	1.01, d (6.9)
17	21.5	1,00, d (2.5)	21.4	1.02, d (6.9)
18	21.9	0,85, s	21.8	0.86, s
19	14.3	0,87, s	33.3	0.90, s
20	19.8	0,98, s	19.7	1.00, s

Relative stereochemistry determined through NOE correlations. **26** is given in (*+*)-configuration consistent with biosynthesis through (*+*)-CPP and accumulation of miltiradiene of this absolute stereochemistry in the native plant species *Coleus forskohlii* and specificity of the biosynthetic enzymes CfTPS1 and CfTPS3.[1]

Supplementary table S8: NMR data of syn-isopimara-9(11),15-diene[a] (6) acquired in chloroform-d_1.

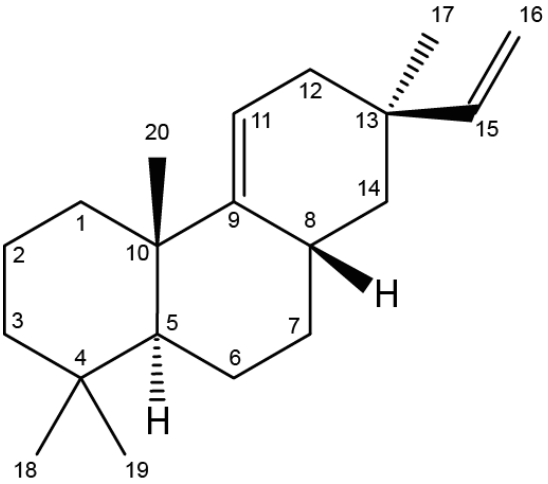

Position	[24]	This work	This work
	δ_H (*J* in Hz)	δ_C	δ_H (*J* in Hz)
1		37.8	1.36,m 1.65, m
2		19.2	1.53,m 1.65, m
3		42.5	1.16,td(13.6,3.9) 1.40, m
4		33.8	
5		53.9	0.95, dd (12.3, 2.6)
6		22.12	1.46,m 1.66, m
7		36.4	1.01, m 1.89, m
8		31.3	2.28, m
9		149.9	
10		39.4	
11	5.29, m	112.6	5.27, ddd (6.1, 2.0, 1.5)
12		37.5	1.72, m 2.05, ddd (17.1, 2.8, 2.0)
13		34.9	
14		42.8	1.10, dd (12.6, 10.9) 1.50, m
15	5.77, dd (17.2, 11.2)	150.5	5.82, dd (17.5, 10.8)
16	4.85–4.93, m	109.3	4.87,dd (10.8, 1.4) 4.94, dd (17.5, 1.4)
17	0.95, s	22.2	0.92, s
18[b]	0.84, s	33.5	0.85, s
19[b]	0.84, s	22.09	0.86, s
20	0.98, s	21.1	1.04, s

[a]Relative stereochemistry concluded on the basis of NOE correlations between H-8 – H-20 and H-8 – H-17 as well as the absence of correlations between H-5 and H-20. [b]Interchangeable. The class II diTPS OssynCPS dicates the stereochemical configuration of C-10 (*S*) and C-5 (*R*),[5] permitting to establish the absolute configuration of **6**.

Supplementary table S9: Diterpene production in *Saccharomyces cerevisiae* using selected natural and new-to-nature diTPS combinations.

#	Compound	Strain	Combination	Yield (mg L^{-1})
23a	(*+*)-manool	EFSC4725	CfTPS1/SsSCS	311 ± 2
25	miltiradiene	EFSC4691	CfTPS1/CfTPS3	250 ± 2
16a	(13*R*,9*S*,10*S*)-manoyl oxide	EFSC4494	CfTPS2/CfTPS3	368 ± 1
20	(13*S*,9*R*,10*R*)-manoyl oxide	EVST20805	TwTPS21/EpTPS1	329 ± 1

Material and Methods

Reagents

All chemicals were acquired from Sigma-Aldrich unless otherwise stated. Authentic standards of abietadiene, sandaracopimaradiene, dehydroabietadiene, neoabietadiene and pimaradiene were prepared as previously described.[11] (+)-Manool was purchased from Callaghan Innovation, NZ. Preparation of the authentic standard of (13*R*)-(+)-manoyl oxide was previously described.[25]

Construction of expression plasmids

All genes used in this work are listed in supplementary table S1. ZmAN2 and Ossyn-CPP were kindly provided by Prof. Reuben Peters (Iowa State University, Ames, USA), SsLPPS, SsSCS MvCPS1 and MvELS5 were described earlier.[3-4] Full length coding sequences for TwTPS7, TwTPS14, TwTPS21, TwTPS28, EpTPS8, EpTPS23 and TwTPS2 were amplified from cDNA[2] using the primers listed in supplementary table S8 and sequence verified. Sequences encoding *Coleus forskohlii* 1-deoxy-d-xylulose 5-phosphate synthase (CfDXS) and geranylgeranyl diphosphate synthase (CfGGPPS) were identified and cloned from cDNA of *C. forskohlii* root cork tissue.[26] For transient expression in *Nicotiana benthamiana*, diTPSs, *CfDXS* and *CfGGPPS* were cloned into the pCAMBIA130035Su[27] plasmid by USER cloning,[28] using primers listed in supplementary table S8.

Transient expression in *Nicotiana benthamiana*

For functional characterization of combinations of diTPSs and identification of pairs yielding diterpene products, enzymes were transiently expressed in the *N. benthamiana*/Agrobacterium system. This platform offers several advantages over microbial hosts including (1) native codon usage, (2) presence of plastids, the subcellular compartment for localization of diTPS and synthesis of the common precursor GGPP, (3) no requirement for sterile culture conditions and (4) efficient co-expression of multiple proteins. Product accumulation occurs within a timeframe comparable to microbial systems (Fig. S5) and can be scaled for yields permitting structure elucidation.

pCAMBIA130035Su constructs carrying diTPS coding sequences and the expression plasmid with the anti-post transcriptional gene silencing protein p19[8] were transformed into the Agrobacterium strain AGL-1 - GV3850 as previously described.[29] For infiltration, the OD_{600} of all Agrobacterium strains was normalized to OD_{600} of 1. Strains of Agrobacterium containing the pCAMBIA130035Su harboring the combinations of class II and I diTPS were mixed with the strain carrying the vector for p19. As controls, mixtures of strains with either class II diTPS or class I diTPS with p19 were used; infiltrations with p19 alone represented the negative control, resulting in a total of 121 specific combinations (supplementary Fig. S1). Agrobacterium suspensions were infiltrated into 4-6 weeks old *N. benthamiana* plants. Plants were grown for an additional 7 d in the greenhouse before extraction of metabolites as described previously.[29] Two leaf discs of 2 cm diameter (approximately 0.2 g fresh weight (FW)) were cut in triplicates from the infiltrated leaves. Diterpenes were extracted in 1 mL n-hexane with 1 mg/L 1-eicosene as internal standard (IS) at room temperature for 1

h in an orbital shaker at 220 rpm. Each combination was repeated at least once, with three experimental replicates. Plant material was collected by centrifugation and the organic phase transferred to GC vials for analysis.

Biosynthesis of selected diterpenes in *Nicotiana benthamiana* for NMR analysis

Several diTPS combinations in *N. benthamiana* resulted in products with intriguing structures. To further exploit the *N. benthamiana* system, several modifications to the experimental setup of the *N. benthamiana* system were established, to reach diterpene levels sufficient for structural analysis by NMR. *Syn*-manool (**11**), *ent*-manool (**23b**), 13*S*-*ent*-manoyl oxide (**16b**) and kolavelool (**26**) in amounts amenable for NMR analysis, were obtained from heterologous expression in *N. benthamiana* of the new-to-nature combinations OssynCPS/SsSCS, ZmAN2/SsSCS, TwTPS21/CfTPS3, and TwTPS14/SsSCS. These diTPS combinations were individually co-expressed with CfDXS and CfGGPPS. Co-expression of CfDXS and CfGGPPS together with CfTPS2/CfTPS3 was shown to efficiently increase biosynthesis of 13*R*-(*+*)-manoyl oxide (**16a**) (supplementary Fig. S2). In addition to co-expressing CfDXS and CfGGPPs, biosynthesis of **11**, **23b**, **16b** and **26a** was scaled up 500-fold by infiltrating over 30 *N. benthamiana* plants (approximately 100 g FW leaf material). Cultures of agrobacterium strains (500 mL) containing plasmids with the constructs for OssynCPS, SsSCS, ZmAN2, TwTPS21, CfTPS3 and TwTPS14, were grown overnight from 20 mL starter cultures and pelleted by centrifugation. Cell pellets were resuspended in dH_2O and adjusted to an OD_{600} of 0.5. Resuspended agrobacteria strains were mixed according to the selected combinations together with strains harboring CfDXS and CfGGPPS. *N. benthamiana* plants were submerged in the Agrobacterium suspensions and vacuum-infiltrated at 50-100 mbar for 30 sec, similar to a method previously described.[30] Leaves were harvested after 7-8 d and cut into small pieces before extraction in 500 mL n-hexane. Solvent was evaporated and recovered by rotary evaporation for three repeated extractions of the same leaf material. Concentrated extracts from *N. benthamiana* biosynthesizing the selected diterpenes were subjected to silica gel column chromatography (SPE), eluted with three fractions of n-hexane and ethyl acetate (100:0, 99:1, 98:2, and 94:6). Fractions containing diterpenes products were identified by GC-MS, combined and the solvent was removed by rotary evaporation before the samples were resuspended in 1 mL n-hexane, yielding a crude fraction for further purification.

In vitro assay for confirmation of biosynthetic products from selected diTPS combinations

To confirm the biosynthetic products obtained in *N. benthamiana*, diTPS combinations were tested in in vitro assays as previously described.[11] In brief, His_6-tagged OsCPSsyn, TwTPS7, ZmAN2, TwTPS21, TwTPS14, EpTPS23, CfTPS3, EpCPS1 and SsSCS were cloned in pET-28a(+) (EMD Biosciences), expressed and purified from *E. coli*. Pairs of class II and class I diTPS were coupled for the *in vitro* assays and the assays were extracted with hexane before analysis.

Production of selected diterpenes in *Saccharomyces cerevisiae*

To demonstrate feasibility of producing the industrially relevant and representative diterpenes with diverse structural features, *syn*-pimara-9,(11),15-diene (**6**), (13*R*)-(*+*)-manoyl oxide (**16a**), (13*R*)-*ent*-manoyl oxide (**20b**), (*+*)-manool (**23a**) and miltiradiene (**25**) were selected for production in yeast (*Saccharomyces cerevisiae*). The combinations of diTPSs introduced into yeast for production of **16a**, **20b**, **23a**, and **25**, can be found in table S9. For the biosynthesis of **6**,

production levels were not achieved (less than 10 mg L^{-1}) from the combination of OssynCPS/CfTPS3. However, the yield from large scale cultures was sufficient for NMR analysis (supplementary table S8). Coding sequences of diTPS genes were optimized for expression in *S. cerevisiae* (Geneart, Life Technologies) and N-terminally truncated to generate pseudo-mature variants lacking plastidial target signals. Truncation sites were predicted using the ChloroP-software[31] at default settings and protein alignments. All recombinant class I diTPSs were expressed driven by the constitutive TDH3-promoter, whereas expression of class II diTPSs was driven by the constitutive TEF1-promoter.[32] DiTPSs used for producing the selected diterpenes (table 1) were integrated into the defined locus XI-5[33] in the *S. cerevisiae* background EFSC4416 (MATa, HO::KO, Δhis3::HIS3, Δleu2::LEU2, Δura3). Strains were selected by uracil/uridine autotrophy on plates containing yeast synthetic complete (SC) media lacking uracil and confirmed by genotyping. Verified transformants were grown in 500 µl selective media (SC-ura) for 16 h at 30°C and 400rpm prior to transfer into Feed In Time (FIT) fed-batch media (m2p-labs, Aachen, Germany) containing 0.8% FIT enzyme mix (50 µL pre-culture to a total volume of 500 µL, 1:10 dilution) for functional assays. Cultures were grown for 72 h at 30°C and 400 rpm in 1.6 mL microtiter plates. For quantification of diterpene production, cultures were freeze-dried and extracted with 2 mL of GC grade n-hexane with 20 mg L^{-1} 1-eicosene as internal standard.

Scale-up of *S. cerevisiae* cultures and purification of diterpenes

To demonstrate scalability in *S. cerevisiae,* production of the diterpenes **6**, **16a**, **20**, **23a** and **25** was transferred from microtiter plate format to shake flask. Strains listed in table 1 and EFSC4690 were inoculated into a pre-culture of 5 ml selective media (SC-Ura) and grown for 16 h at 30°C and 400rpm. Pre-cultures of 5 mL were inoculated into FIT media containing 0.8 % FIT enzyme mix and grown for 72 h at 30°C. Four cultures were combined and yeast cells were harvested by centrifugation (2000*g*, 5 min, 4°C) and re-suspended in 200 mL deionized water. Diterpenes were extracted with 200 ml UV-grade ethanol (99.9%) at 60°C for 20 min. The organic phase was cleared of cell-debris by centrifugation (3,600*g*, 5 min, 4°C) and partitioned with 100 mL n-hexane by horizontal shaking at 200 rpm for 1 h. The hexane phase was concentrated by rotary evaporation and subjected to column chromatography (dual layer Florisil/Na_2SO_4 6mL PP SPE TUBE, Supelco Analytical) with a gradient of n-hexane and 1-15% ethyl acetate. Fractions containing the desired diterpenes were identified by GC-MS, combined the solvent was removed by rotary evaporation. The purity of the diterpenes was sufficient for NMR analysis after this single purification step.

GC-MS analysis of diterpenes biosynthesized in *Nicotiana benthamiana*

Extracts of the 121 diTPS combinations and their respective controls were analyzed on a Shimadzu GCMS-QP2010 Ultra using an Agilent HP-5MS column (30 m x 0.25 mm i.d., 0.25 µm film thickness). Injection volume and temperature was set at 1 µL and 250°C with the following GC program: 50°C for 2 min, ramp at rate 4°C min^{-1} to 110°C, ramp at rate 8°C min^{-1} to 250°C, ramp at rate 10°C min^{-1} to 310°C and hold for 5 min. Kovat's retention indices of component peaks were calculated by referring to index standard peaks of 1 ppm C7 - C30 saturated alkanes as reference, based on the programmed temperature analysis (linear RI) with the GCMSsolution version 2.70 software package (LabSolutions). The ion source temperature of the mass spectrometer (MS) was set to 230°C and spectra were recorded from m/z 50 to m/z

350. Compound identification was carried out using authentic standards and comparison to reference spectra in databases (Wiley Registry of Mass Spectral Data, 8th Edition, July 2006, John Wiley & Sons, ISBN: 978-0-470-04785-9) (see supplementary table 1). Quantification was based on the average of the experimental replicates of the total ion chromatogram (TIC) peak area normalized to the TIC area of IS.

For separation of stereoisomers, diterpenes were separated on a chiral column (Supelco Beta DEX^{TM} 120 (30 m x 0.25 mm i.d., 0.25 µm film thickness). Injection volume and temperature was set to 1 µL and 230°C. GC program: 100°C for 3 min, ramp at rate 20°C min^{-1} to 155°C, ramp at rate 0.2°C min^{-1} to 190°C, ramp at rate 20°C min^{-1} to 230°C and hold for 7 min. The ion source temperature was set to 280°C and spectra were recorded from m/z 50 to m/z 300. Identification of diterpenes was based on their characteristic mass spectrum and authentic standards.

Purification of *syn*-manool (11), (13*S*)-*ent*-manoyl oxide (16b), *ent*-manool (23b) and kolavelool (26a) from SPE purified *Nicotiana benthamiana* extracts.

Due to the efficient formation of potentially structurally intriguing diterpene backbones in combinations of diTPSs, **11, 23b, 26a, 16b** were selected for further purification from the up-scaled *N. benthamiana* expression for structural elucidation. With the exception of (13*S*)-*ent*-manoyl oxide (**16b**), the SPE purified diterpenes from the *N. benthamiana* extracts were further purified on a HPLC-HRMS-SPE-NMR system to obtain purity amenable for NMR. The HPLC-HRMS-SPE-NMR system consisted of an Agilent 1200 chromatograph comprising quaternary pump, degasser, thermostated column compartment, autosampler, and photodiode array detector (Santa Clara, CA), a Bruker micrOTOF-Q II mass spectrometer (Bruker Daltonik, Bremen, Germany) equipped with an electrospray ionization source and operated via a 1:99 flow splitter, a Knauer Smartline K120 pump for post-column dilution (Knauer, Berlin, Germany), a Spark Holland Prospekt2 SPE unit (Spark Holland, Emmen, The Netherlands), a Gilson 215 liquid handler equipped with a 1 mm needle for automated filling of 1.7 mm NMR tubes, and a Bruker Avance III 600 MHz NMR spectrometer (^{1}H operating frequency 600.13 MHz) equipped with a Bruker SampleJet sample changer and a cryogenically cooled gradient inverse triple-resonance 1.7 mm TCI probe-head (Bruker Biospin, Rheinstetten, Germany). Mass spectra were acquired in positive ionization mode, using a drying temperature of 200°C, capillary voltage of 4100 V, nebulizer pressure of 2.0 bar, and drying gas flow of 7 L min^{-1}. A solution of sodium formate clusters was automatically injected at the beginning of each run for internal mass calibration. Cumulative SPE trapping of diterpenes was performed with 10 consecutive separations using a chromatographic method as follows: 0 min, 90% B; 15 min, 100% B; 20 min, 100% B; 25 min, 100% B; 26 min, 90% B with 10 min equilibration prior to injection of 5 µL pre-fractionated sample (8.5 mg mL^{-1} in hexane). The HPLC eluate was diluted with Milli-Q water at a flow rate of 1.0 mL min^{-1} prior to trapping on 10 × 2 mm i.d. Resin GP (general purpose, 5-15 µm, spherical shape, polydivinyl-benzene phase) SPE cartridges (Spark Holland, Emmen, The Netherlands), and diterpenes were trapped using threshold of a UV chromatogram at 205 nm. The SPE cartridge was dried with pressurized nitrogen gas for 60 min prior to elution with chloroform-*d*. The HPLC was controlled by Bruker Hystar version 3.2 software, automated filling of NMR tubes were controlled by PrepGilsonST version 1.2 software, and

automated NMR acquisition were controlled by Bruker IconNMR version 4.2 software. NMR data processing was performed using Bruker Topspin version 3.2 software.

For purification of **16b**, the SPE fraction containing **16b** was resuspended in 1 mL dichloromethane and applied on a gel filtration column, (Sephadex^{TM} LH-20, GE healthcare), conditioned in dichloromethane. The column efflux was fractionated by an automated fraction collector, and the solvent in fractions containing **16b** was removed under an air stream. This purification procedure was repeated three times, to obtain purity of **16b** suitable for NMR analysis.

NMR analysis

To determine the structure and relative stereochemistry of **6**, **11**, **16a**, **16b**, **20b**, **23a**, **23b**, **25** and **26** these diterpenes were subjected to NMR analysis. The NMR spectra of **11**, **23b**, **26** were recorded in chloroform-d_1 at 300 K on the above-mentioned instrument. ^{1}H and ^{13}C chemical shifts were referenced to the residual solvent signal (δ 7.26 and δ 77.16, respectively). One-dimensional ^{1}H NMR spectra were acquired in automation (temperature equilibration to 300 K, optimization of lock parameters, gradient shimming, and setting of receiver gain) with 30°-pulses, 3.66 s inter-pulse intervals, 64k data points and multiplied with an exponential function corresponding to line-broadening of 0.3 Hz prior to Fourier transform. Phase-sensitive DQF-COSY and NOESY spectra were recorded using a gradient-based pulse sequence with a 20 ppm spectral width and 2k x 512 data points (processed with forward linear prediction to 1k data points). Multiplicity-edited HSQC spectrum was acquired with the following parameters: spectral width 20 ppm for ^{1}H and 200 ppm for ^{13}C, 2k x 256 data points (processed with forward linear prediction to 1k data points), and 1.0 s relaxation delay. HMBC spectra were optimized for $^{n}J_{C,H}$ = 8 Hz and acquired using the following parameters: spectral width 20 ppm for ^{1}H and 240 ppm for ^{13}C, 2k x 128 data points (processed with forward linear prediction to 1k data points), and 1.0 s relaxation delay.

NMR spectra of **6**, **16a**, **16b**, **20b**, **23a**, and **25** were recorded in chloroform-*d* at 300 K on a Bruker Avance III 600 MHz NMR spectrometer (^{1}H operating frequency 600.13 MHz) equipped with a Bruker SampleCase sample changer and a cryogenically cooled gradient 5.0 mm DCH probe-head (Bruker Biospin, Rheinstetten, Germany) in a 3.0 mm o.d. NMR tube. ^{1}H and ^{13}C chemical shifts were referenced to the residual solvent signal (δ 7.26 and δ 77.16, respectively). One-dimensional ^{1}H and ^{13}C NMR spectra were acquired in automation (temperature equilibration to 300 K, optimization of lock parameters, gradient shimming, and setting of receiver gain) with 30°-pulses, 3.66 sec inter-pulse intervals, 64k data points and multiplied with an exponential function corresponding to line-broadening of 0.3 and 1.0 Hz, respectively prior to Fourier transform. Phase-sensitive DQF-COSY and ROESY spectra were recorded using a gradient-based pulse sequence with a 7.4 ppm spectral width and 2k x 128 and 2k x 256 data points, respectively (processed with forward linear prediction to 1k data points). Multiplicity-edited HSQC spectrum was acquired with the following parameters: spectral width 16 ppm for ^{1}H and 165 ppm for ^{13}C, 2k x 256 data points (processed with forward linear prediction to 1k data points), and 1.0 sec relaxation delay. HMBC spectra were optimized for $^{n}J_{C,H}$ = 8 Hz and acquired using the following

parameters: spectral width 7.9 ppm for ^{1}H and 221 ppm for ^{13}C, 4k x 256 data points (processed with forward linear prediction to 1k data points), and 1.0 sec relaxation delay.

Optical rotation experiments

To determine the absolute stereochemistry of **16a**, **16b**, **20b** and **23a**, an optical rotation measurement and comparison to literature values was performed. The optical rotation was measured on a Bellingham and Stanley Ltd ADP410 polarimeter using a 0.5 dm sample cell at D-line (589 nm).

Quantification of diterpenes produced in *Saccharomyces cerevisiae*

Since production of complex diterpenes is the ultimate goal of this work, the levels of diterpenes accumulating in *S. cerevisiae* in microtiter plate assays were determined. Quantification of **16a**, **20b**, **23a** and **25** was carried out using a SCION 436 GC-FID (Bruker). Sample volumes of 3 µL were injected in splitless mode at 250°C with the following GC-program: 60°C for 1 min, ramp at rate 30°C min^{-1} to 180°C, ramp at rate 10°C min^{-1} to 250°C, ramp at rate 30°C min^{-1} to 320°C and hold for 2 min. H_2 was used as carrier gas with a linear flow of 50mL min^{-1}. The FID was set at 300°C, with a N_2 flow of 25 mL min^{-1}, H_2 at 30mL min^{-1} and air 300 mL min^{-1}. Data sampling rate was 10 Hz. Diterpenes were identified by retention time and comparison to authentic standards. Quantification of diterpenes was carried out by integration of their peak area, normalized to the peak area of 20 mg/L 1-eicosene (IS) and by comparison with the authentic standard **16a**[25] and the relative response factor set to 1, as determined experimentally.

Primers

Supplementary table S10: Primer list

Name	sequence	Gene of Interest
Amplification of full length genes from cDNA synthesized from plant tissues total RNA		
TwTPS7_F	GGTCGCAAGTTAGAGCATATGCATAG	TwTPS7
TwTPS7_R	CATCAACAGTGTTAATCTACTCTCTCA	TwTPS7
TwTPS14/21_F	CAAAGCCAATCAATCATGTTCATGTCC	TwTPS14
TwTPS14/21_R	GATCTTATACTACTCTTTCAAAGAGTACTTTGGC	TwTPS14
TwTPS14/21_F	CAAAGCCAATCAATCATGTTCATGTCC	TwTPS21
TwTPS14/21_R	GATCTTATACTACTCTTTCAAAGAGTACTTTGGC	TwTPS21
TwTPS14/21_F	CAAAGCCAATCAATCATGTTCATGTCC	TwTPS28
TwTPS14/21_R	GATCTTATACTACTCTTTCAAAGAGTACTTTGGC	TwTPS28
EpTPS8_F	GCAGACGCCAATCTTTCTTGGT	EpTPS8
EpTPS8_R	TTATGAAGTTAAAAGGAGTGGTTCGTTGAC	EpTPS8
EpTPS23_F	CCGATCTCCTGCATTAAACTCGACA	EpTPS23
EpTPS23_R	TCTATGGCATGAGAAGTGGGTCCT	EpTPS23
TwTPS2_F	GAATTTATGGTAGAATGTCAGTATTTATCAAATCG	TwTPS2
TwTPS2_R2	TGCAATTATAGAGAGATGGGTTCACG	TwTPS2
F_CfDXS2	ATGGCGTCTTGTGGAGCTA	CfDXS
R_CfDXS2	TTACATGTTGATCAAATGAAGACTG	CfDXS
F_CfGGPPs1	TCATCAAGCAGAGCAAACTA	CfGPPS
R_CfGGPPs1	ACTACACAAAGCCCCTAAGA	CfGPPS
Cloning of full length diTPS genes into pCAMBIA130035Su for transient expression in *N. benthamiana*		
TwTPS7_5'	GGCTTAA/ideoxyU/ATGCATAGTTTGTTAATGAAA	TwTPS7
TwTPS7_3'	GGTTTAA/ideoxyU/TTAATCTACTCTCTCAAAGAGTACTTTGGCAAT	TwTPS7
TwTPS14_21_28_5'	GGCTTAA/ideoxyU/ATGTTCATGTCCTCCTCCTCCTCTTCTC	TwTPS14,TwTPS21,TwTPS28

TwTPS14_21_28_3'	GGTTTAA/ideoxyU/TTATACTACTCTTTCAAAGAGTACTTTGGCAAT	TwTPS14,TwTPS21,TwTPS28
oSSB184	GGCTTAA/ideoxyU/ATGCAAGTCTCTCTCCCTCAC	EpTPS8
oSSB185	GGTTTAA/ideoxyU/TTAAAGGAGTGGTTCGTTGACAATT	EpTPS8
EpTPS23_5'	GGCTTAA/ideoxyU/ATGTTATTGGCTAGTTCTACCTCTTCG	EpTPS23
EpTPS23_3'	GGTTTAA/ideoxyU/CTATGGCATGAGAAGTGGGTCC	EpTPS23
TwTPS2_5'	GGCTTAA/ideoxyU/ATGTTTGATAAGACCCAACTC	TwTPS2
TwTPS2_3'	GGTTTAA/ideoxyU/TTATAGAGAGATGGGTTCACGTATCAAAGCGTT	TwTPS2
XwP1	GGCTTAA/ideoxyU/ATGACTTCTGTAAATTTGAGC	SsLPPS
XwP5	GGTTTAA/ideoxyU/TTATACAACCGGTCGAAAGAGTAC	SsLPPS
XwP6	GGCTTAA/ideoxyU/ATGTCGCTCGCCTTCAAC	SsSCS
XwP2	GGTTTAA/ideoxyU/TCAAAAGACAAAGGATTTCATATC	SsSCS
ZmAN2_5'	GGCTTAA/ideoxyU/ATGGTTCTTTCATCGTCTTGCACAA	ZmAN2
ZmAN2_3'	GGTTTAA/ideoxyU/TTATTTTGCGGCGGAAACAGGTTCA	ZmAN2
syn-CPP_5'	GGCTTAA/ideoxyU/ATGCCGGTCTTCACTGCGT	OsCPSsyn
syn-CPP_3'	GGTTTAA/ideoxyU/TTAAATCACATCTTGGAATATGACCTTGTCGAT	OsCPSsyn
CfDXS2_5'	GGCTTAA/ideoxyU/ATGGCGTCTTGTGGAGCTATCGGGAGTAG	CfDXS
CfDXS2_3'	GGTTTAA/ideoxyU/TTACATGTTGATCAAATGAAGACTGTCTTTCC	CfDXS
CfGGPPs2_5'	GGCTTAA/ideoxyU/ATGAGGTCTATGAATCTGGTCGATGCTT	CfGPPS
CfGGPPs2_3'	GGTTTAA/ideoxyU/TTAGTTCTGCCTGTGAGCAATGTAATCGGCCAG	CfGPPS

Cloning of pseudomature diTPS genes into pET28b+ for *E. coli* expression

EpTPS8_NcoI_pmF	CAAGTCTCCATGGCCCTCACCAC	EpTPS8
EpTPS8_XhoI_R	CTAGAAACTCGAGTGAAGTTAAAAGGAGTG	EpTPS8
EpTPS23_BspHI_pmF	GGAAGTGTTCTCATGAAGCTGAGCCA	EpTPS23
EpTPS23_XhoI_R	AGCTCGAGTGGCATGAGAAGTGG	EpTPS23
TwTPS7_NcoI_inFusion_F	AGGAGATATACCATGAGTGGCCACGGTGC	TwTPS7
TwTPS7_XhoI_inFusion_R	GTGGTGGTGCTCGAGATCTACTCTCTCAAA	TwTPS7
Tw CPS inFusion_F	AGGAGATATACCATGGGCATTGCAAAATCCAAGCCT	TwTPS14,TwTPS21,TwTPS28
Tw CPS inFusion_R	GGTGGTGGTGCTCGAGTACTACTCTTTCAAAGAGTAC	TwTPS14,TwTPS21,TwTPS28
SsLPPS InFusion-F	AGGAGATATACCATGGCTGAATTGAGAGTAACAAGCCTG	SsLPPS
SsLPPS InFusion-R	GGTGGTGGTGCTCGAGTACAACCGGTCGAAAGAGTACTTTG	SsLPPS
ZmAN2 InFusion-F	AGGAGATATACCATGGCCCAGCACACCAGCGAATC	ZmAN2
ZmAN2 InFusion-R	GGTGGTGGTGCTCGAGTTTTGCGGCGGAAACAGGTTC	ZmAN2
OsSynCPP in Fusion-F	AGGAGATATACCATGCCGGCCTCGGAAGAAACACG	OsCPSsyn
OsSynCPP in Fusion-R	GGTGGTGGTGCTCGAGAATCACATCTTGGAATATGACCTTG	OsCPSsyn

Cloning of pseudomature diTPS genes for introduction into *S. cerevisae*

TwTPS21_ COfwdU	AGCGATACGUAAAAATGGGTATCGCTAAATCCAAGC	TwTPS21
TwTPS21_ CORevU	CACGCGAUTCAGTGATGGTGATGATGATGTTC	TwTPS21
EpTPS1_ COfwdU	CGTGCGAUTTAGTGATGGTGATGATGATGTTC	EpTPS1
EpTPS1_ CORevU	ATCAACGGGUAAAAATGGCTCAATCCGTTGCTGAATCC	EpTPS1
CfTPS2_COfwdU	AGCGATACGUAAAAATGTCCAGAGTTGCTTCCTTGG	CfTPS2
CfTPS2_CORevU	CACGCGAUTTAAACAACAGGTTCGAACAAAACTTGG	CfTPS2
CfTPS3_COfwdU	ATCAACGGGUAAAAATGATCACCTCCAAATCTTCC	CfTPS3
CfTPS3_CORevU	CGTGCGAUTCAGTTACTGACGCAGGAC	CfTPS3
CfTPS1_ COfwdU	AGCGATACGUAAAATGGCTTGGATGAACAACGGTAAG	CfTPS1
CfTPS1_ CORevU	CACGCGAUTCAGGCGACTGGTTCGAAC	CfTPS1
SsSCS _ COfwdU	ATCAACGGGUAAAATGGCCAAGATGAAGGAAAACTTCAA	SsSCS
SsSCS_ CORevU	CGTGCGAUTTAAAAAACGAAGGACTTCATATCTTC	SsSCS
OssynCPP_ COfwdU	AGCGATACGUAAAATGCCGGCCTCGGAAGAAACA	OsCPSsyn
OssynCPP_ CORevU	CACGCGAUCTAAATCACATCTTGGAATATGACCTTGTC	OsCPSsyn

References

[1] I. Pateraki, J. Andersen-Ranberg, B. Hamberger, A. M. Heskes, H. J. Martens, P. Zerbe, S. S. Bach, B. L. Møller, J. Bohlmann, B. Hamberger, *Plant Physiol.* **2014**, *164*, 1222-1236.

[2] P. Zerbe, B. Hamberger, M. M. S. Yuen, A. Chiang, H. K. Sandhu, L. L. Madilao, A. Nguyen, B. Hamberger, S. S. Bach, J. Bohlmann, *Plant Physiol.* **2013**, *162*, 1073-1091.

[3] A. Caniard, P. Zerbe, S. Legrand, A. Cohade, N. Valot, J.-L. Magnard, J. Bohlmann, L. Legendre, *BMC Plant Biol.* **2012**, *12*, 119.
[4] P. Zerbe, A. Chiang, H. Dullat, M. O'Neil-Johnson, C. Starks, B. Hamberger, J. Bohlmann, *The Plant Journal* **2014**, *79*, 914-927.
[5] M. Xu, M. L. Hillwig, S. Prisic, R. M. Coates, R. J. Peters, *Plant J.* **2004**, *39*, 309-318.
[6] L. J. Harris, A. Saparno, A. Johnston, S. Prisic, M. Xu, S. Allard, A. Kathiresan, T. Ouellet, R. J. Peters, *Plant Mol. Biol.* **2005**, *59*, 881-894.
[7] L. W. Sumner, A. Amberg, D. Barrett, M. H. Beale, R. Beger, C. A. Daykin, T. W. Fan, O. Fiehn, R. Goodacre, J. L. Griffin, T. Hankemeier, N. Hardy, J. Harnly, R. Higashi, J. Kopka, A. N. Lane, J. C. Lindon, P. Marriott, A. W. Nicholls, M. D. Reily, J. J. Thaden, M. R. Viant, *Metabolomics* **2007**, *3*, 211-221.
[8] O. Voinnet, S. Rivas, P. Mestre, D. Baulcombe, *Plant J.* **2003**, *33*, 949-956.
[9] K. Zhou, M. Xu, M. Tiernan, Q. Xie, T. Toyomasu, C. Sugawara, M. Oku, M. Usui, W. Mitsuhashi, M. Chono, P. M. Chandler, R. J. Peters, *Phytochemistry* **2012**, *84*, 47-55.
[10] K. Bruckner, A. Tissier, *Plant Methods* **2013**, *9*, 46.
[11] B. Hamberger, T. Ohnishi, B. Hamberger, A. Seguin, J. Bohlmann, *Plant Physiol.* **2011**.
[12] J. Zi, R. J. Peters, *Organic & Biomolecular Chemistry* **2013**, *11*, 7650-7652.
[13] M. T. Nielsen, J. Andersen-Ranberg, U. Christensen, M. Kristensen, S. J. Harrison, C. E. Olsen, B. Hamberger, B. L. Møller, M. H. H. Nørholm, *unpublised* **2014**.
[14] K. Potter, J. Criswell, J. Zi, A. Stubbs, R. J. Peters, *Angew. Chem. Int. Ed.* **2014**, *53*, 7198-7202.
[15] aN. Totté, L. Charon, M. Rohmer, F. Compernolle, I. Baboeuf, J. M. C. Geuns, *Tetrahedron Lett.* **2000**, *41*, 6407-6410; bJ.-L. Li, Q.-Q. Chen, Q.-P. Jin, J. Gao, P.-J. Zhao, S. Lu, Y. Zeng, *Phytochemistry* **2012**, *76*, 32-39.
[16] aD. M. Martin, J. Fäldt, J. Bohlmann, *Plant Physiol.* **2004**, *135*, 1908-1927; bC. I. Keeling, S. Weisshaar, R. P. C. Lin, J. Bohlmann, *Proceedings of the National Academy of Sciences* **2008**, *105*, 1085-1090; cD. E. Hall, P. Zerbe, S. Jancsik, A. L. Quesada, H. Dullat, L. L. Madilao, M. Yuen, J. Bohlmann, *Plant Physiol.* **2013**, *161*, 600-616.
[17] M. Schalk, L. Pastore, M. A. Mirata, S. Khim, M. Schouwey, F. Deguerry, V. Pineda, L. Rocci, L. Daviet, *J. Am. Chem. Soc.* **2012**, *134*, 18900-18903.
[18] M. T. Nielsen, J. A. Ranberg, U. Christensen, H. B. Christensen, S. J. Harrison, C. E. Olsen, B. Hamberger, B. L. Moller, M. H. Norholm, *Appl. Environ. Microbiol.* **2014**, *80*, 7258-7265.
[19] C. Demetzos, A. Kolocouris, T. Anastasaki, *Bioorg. Med. Chem. Lett.* **2002**, *12*, 3605-3609.
[20] G. Topcu, E. N. Altiner, S. Gozcu, B. Halfon, Z. Aydogmus, J. M. Pezzuto, B.-N. Zhou, D. G. Kingston, *Planta Med.* **2003**, *69*, 464-467.
[21] T. Hoshino, C. Nakano, T. Ootsuka, Y. Shinohara, T. Hara, *Organic & Biomolecular Chemistry* **2011**, *9*, 2156-2165.
[22] C. Demetzos, A. Kolocouris, T. Anastasaki, *Bioorg. Med. Chem. Lett.* **2002**, *12*, 3605-3609.
[23] M. D. Bomm, J. Zukerman-Schpector, L. M. X. Lopes, *Phytochemistry* **1999**, *50*, 455-461.
[24] H. Oikawa, H. Toshima, S. Ohashi, W. A. König, H. Kenmoku, T. Sassa, *Tetrahedron Lett.* **2001**, *42*, 2329-2332.
[25] M. T. Nielsen, J. Andersen-Ranberg, U. Christensen, H. B. Christensen, S. J. Harrison, C. E. Olsen, B. Hamberger, B. L. Møller, M. H. H. Nørholm, *Applied and Environmental Microbiology* **2014**.
[26] I. Pateraki, J. Andersen-Ranberg, B. Hamberger, A. M. Heskes, H. J. Martens, P. Zerbe, S. S. Bach, B. L. L. Møller, J. Bohlmann, B. Hamberger, *Plant Physiology* **2014**.
[27] H. H. Nour-Eldin, B. G. Hansen, M. H. H. Nørholm, J. K. Jensen, B. A. Halkier, *Nucleic Acids Res.* **2006**, *34*, e122.
[28] H. Nour-Eldin, F. Geu-Flores, B. Halkier, in *Plant Secondary Metabolism Engineering, Vol. 643* (Ed.: A. G. Fett-Neto), Humana Press, **2010**, pp. 185-200.
[29] S. Spanner Bach, J.-E. Bassard, J. Andersen-Ranberg, M. Emil Møldrup, H. Toft Simonsen, B. Hamberger, in *Methods Mol. Biol.: Plant isoprenoids, Vol. 1153* (Ed.: J. M. Walker), Springer, **2014**, p. 330.
[30] F. Sainsbury, P. Saxena, K. Geisler, A. Osbourn, G. P. Lomonossoff, in *Methods Enzymol., Vol. 517* (Ed.: A. H. David), Academic Press, **2012**, pp. 185-202.
[31] O. Emanuelsson, H. Nielsen, G. V. Heijne, *Protein Sci.* **1999**, *8*, 978-984.
[32] F. Schirmaier, P. Philippsen, *The EMBO Journal* **1984**, *3*, 3311-3315.
[33] M. D. Mikkelsen, L. D. Buron, B. Salomonsen, C. E. Olsen, B. G. Hansen, U. H. Mortensen, B. A. Halkier, *Metab. Eng.* **2012**, *14*, 104-111.